Journal of Scientific Computing (2018) 77:1874–1908
https://doi.org/10.1007/s10915-018-0797-4

Non-conforming Harmonic Virtual Element Method: *h*- and *p*-Versions

Lorenzo Mascotto[1] · Ilaria Perugia[1] · Alexander Pichler[1]

Received: 11 January 2018 / Revised: 7 June 2018 / Accepted: 30 July 2018 / Published online: 22 August 2018

Abstract

We study the h- and p-versions of non-conforming harmonic virtual element methods (VEM) for the approximation of the Dirichlet–Laplace problem on a 2D polygonal domain, providing quasi-optimal error bounds. Harmonic VEM do not make use of internal degrees of freedom. This leads to a faster convergence, in terms of the number of degrees of freedom, as compared to standard VEM. Importantly, the technical tools used in our p-analysis can be employed as well in the analysis of more general non-conforming finite element methods and VEM. The theoretical results are validated in a series of numerical experiments. The hp-version of the method is numerically tested, demonstrating exponential convergence with rate given by the square root of the number of degrees of freedom.

Keywords Virtual element methods · Non-conforming methods · Laplace problem · Approximation by harmonic functions · hp error bounds · Polytopal meshes

Mathematics Subject Classification 65N30 · 65N12 · 65N15 · 35J05 · 31A05

1 Introduction

In recent years, Galerkin methods based on polygonal/polyhedral meshes have attracted a lot of attention, owing to their flexibility in dealing with complex geometries [5,19,31,38,39,41, 55]. In this paper, we focus on the virtual element method (VEM) introduced in [13,16]. The main feature of VEM, in addition to the fact that they allow for general polytopal meshes, is that they are based on trial and test spaces that consist of solutions to local problems mimicking the target one. These functions are not known in a closed form, which is at the origin of the name “virtual”. Importantly, the construction of the method does not rely on

✉ Ilaria Perugia
ilaria.perugia@univie.ac.at

Lorenzo Mascotto
lorenzo.mascotto@univie.ac.at

Alexander Pichler
alex.pichler@univie.ac.at

1 Faculty of Mathematics, University of Vienna, 1090 Vienna, Austria

an explicit representation of the basis functions, but rather on the explicit knowledge of the degrees of freedom. This allows to compute certain projection operators from local VE spaces into polynomial ones, which are instrumental in the definition of proper bilinear forms.

Owing to its flexibility and simplicitity of the implementation, despite its novelty, the basic VEM paradigm has already been extended to highly-regular [22] and non-conforming [7,34] approximating spaces, combined with domain decomposition techniques [27], adaptive mesh refinement [32], adapted to curved domains [23], and applied to a wide variety of problems; among them, we recall general second-order elliptic problems [14], eigenvalue problems [43,53], Stokes problem [21], elasticity problem [15], Helmholtz problem [54], Cahn–Hilliard equation [3], discrete fracture network simulations [24], and topology optimization [42].

In this paper, we introduce and analyze *non-conforming* harmonic VEM for the approximation of the Dirichlet–Laplace problem on polygonal domains. These methods can be seen as the intermediate conformity level between the continuous harmonic VEM developed in [36], and the harmonic discontinuous Galerkin finite element method (DG-FEM) of [45–47]. As typically done in non-conforming methods, instead of requiring C^0-continuity of test and trial functions over the entire physical domain, one only imposes that the moments, up to a certain order, of their jumps across two adjacent elements are zero. We highlight that non-conforming VEM were introduced in [7] for the approximation of the Poisson problem and were subsequently extended to the approximation of general elliptic and Stokes problems in [33,34], respectively. Our method inherits the structure of that of [7], but makes use of harmonic basis functions, which yield to faster convergence, when approximating harmonic solutions, as compared to standard basis functions.

We are particularly interested in the investigation of the h- and p-versions of these methods. In the former version, convergence is achieved by fixing the dimension of local spaces and refining the mesh, whereas, in the latter, by fixing a single mesh and increasing the dimension of local spaces. A combination of the two goes by the name of hp-version. The literature regarding the p- and hp-versions of VEM is restricted to [4,17,18,40,48], in addition to the above-mentioned work [36]; for the hp-version of DG-FEM and hybrid-high order methods on polytopal grids, see [1,31] and the references therein. We derive quasi-optimal error bounds in the broken H^1 norm and in the L^2 norm, which are explicit in terms of the mesh size and of the degree of accuracy of the method. Although not covered by our theoretical analysis, we provide numerical evidence that, similarly as for the harmonic VEM and harmonic DG-FEM [36,45], the exponential convergence of the hp-version of the non-conforming harmonic VEM is faster than the one of standard FEM [8,56] and VEM [17,18].

The tools that we employ in the forthcoming p-analysis of non-conforming harmonic VEM can actually be employed as well in the p-analysis of non-conforming FEM and of non-conforming VEM. For instance, our argument to trace back best approximation estimates by means of non-conforming harmonic VE functions to best approximation estimates by means of discontinuous harmonic polynomials (Proposition 3.1) extends to the non-harmonic case (Proposition 3.8). This provides a useful tool in order to develop a p-analysis of the non-conforming VEM of [7].

We stress that, in the high-order case, the construction of an explicit basis for non-conforming harmonic VEM, as well as for non-conforming standard VEM, is much simpler than for non-conforming FEM, see for instance [37].

The design and analysis of the non-conforming harmonic VEM developed in this paper pave the way for the study of VEM for the Helmholtz problem in a truly Trefftz setting, alternative to the conforming plane wave VEM of [54], which was based on a partition of unity approach. In fact, the non-conforming framework seems to be the most appropriate one in order to design virtual Helmholtz–Trefftz approximation spaces. Such an extension has been investigated in the recent work [49].

The outline of this paper is as follows. In Sect. 2, the model problem is formulated and the concept of regular polygonal decompositions needed for the analysis is introduced; besides, we recall the definition of non-conforming Sobolev spaces subordinated to polygonal decompositions of the physical domain. Section 3 is dedicated to the construction of the 2D non-conforming harmonic VEM and to the analysis of its h- and p-versions; further, a hint for the extension to the 3D case is given. Next, in Sect. 4, numerical results validating the theoretical convergence estimates are presented; a numerical investigation of the full hp-version of the method is also provided. Finally, details on the implementation of the method are given in "Appendix A".

Notation We fix here once and for all the notation employed throughout the paper. Given any domain $D \subseteq \mathbb{R}^d$, $d \in \mathbb{N}$, and $\ell \in \mathbb{N}$, we denote by $\mathbb{P}_\ell(D)$ and $\mathbb{H}_\ell(D)$ the spaces of polynomials and harmonic polynomials up to order ℓ over D, respectively; moreover, we set $\mathbb{P}_{-1}(D) = \mathbb{H}_{-1}(D) = \emptyset$.

We use the standard notation for Sobolev spaces, norms, seminorms and inner products. More precisely, we denote the Sobolev space of functions with square integrable weak derivatives up to order s over D by $H^s(D)$, and the corresponding seminorms and norms by $|\cdot|_{s,D}$ and $\|\cdot\|_{s,D}$, respectively. Sobolev spaces of non-integer order can be defined, for instance, by interpolation theory. In addition, for bounded D, $H^{1/2}(\partial D)$ denotes the space of traces of $H^1(D)$ functions; $H^1_0(D)$ and $H^1_g(D)$ are the Sobolev spaces of H^1 functions with traces equal to zero and equal to a given function $g \in H^{1/2}(\partial D)$, respectively. Further, $(\cdot,\cdot)_{0,D}$ is the usual L^2 inner product over D.

We employ the following multi-index notation: for $\boldsymbol{\alpha} = (\alpha_1, \ldots, \alpha_d)$,

$$\boldsymbol{x}^{\boldsymbol{\alpha}} = x_1^{\alpha_1} x_2^{\alpha_2} \ldots x_d^{\alpha_d}, \quad \partial^{\boldsymbol{\alpha}} = \partial_1^{\alpha_1} \partial_2^{\alpha_2} \ldots \partial_d^{\alpha_d},$$

with $|\boldsymbol{\alpha}| = \alpha_1 + \cdots + \alpha_d$, and where ∂_ℓ^α denotes the α-th partial derivative along direction x_ℓ.

In the sequel, we also use the notation $a \lesssim b$ meaning that there exists a constant $c > 0$, independent of h and p, such that $a \leqslant c\, b$. Finally, we use the notation $a \approx b$ in lieu of $a \lesssim b$ and $b \lesssim a$ simultaneously.

2 Continuous Problem, Polygonal Decompositions and Functional Setting

Here, we want to set the target problem and some basic notation we need for the construction of the non-conforming harmonic virtual element method (VEM). More precisely, the outline of the section is as follows. In Sect. 2.1, we introduce the model problem, that is a Laplace problem on a polygonal domain. Then, in Sect. 2.2, we define the concept of regular decompositions into polygons of the physical domain of the problem. Finally, in Sect. 2.3, we describe non-conforming Sobolev spaces over such polygonal decompositions.

2.1 The Continuous Problem

The target problem we aim to approximate is a Laplace problem over a polygonal domain $\Omega \subset \mathbb{R}^2$ with boundary $\partial\Omega$. More precisely, given $g \in H^{1/2}(\partial\Omega)$, we look for a function u

solving

$$\begin{cases} -\Delta u = 0 & \text{in } \Omega \\ u = g & \text{on } \partial\Omega. \end{cases} \tag{1}$$

The weak formulation of (1) reads

$$\begin{cases} \text{find } u \in V_g \text{ such that} \\ a(u, v) = 0 \quad \forall v \in V_0, \end{cases} \tag{2}$$

where

$$a(u, v) := (\nabla u, \nabla v)_{0,\Omega}, \quad V_g := H^1_g(\Omega), \quad V_0 := H^1_0(\Omega). \tag{3}$$

Well-posedness of problem (2) follows from a lifting argument and the Lax–Milgram lemma.

2.2 Regular Polygonal Decompositions

In this section, we introduce the concept of regular sequences of polygonal decompositions of the domain Ω, which will be needed in the forthcoming analysis of the method.

Let $\{\mathcal{T}_n\}_{n\in\mathbb{N}}$ be a sequence of *conforming* polygonal decompositions of Ω; by conforming, we mean that, for each $n \in \mathbb{N}$, every internal edge e of $\mathcal{T}_n$ is contained in the boundary of precisely two elements in the decomposition. This automatically includes the possibility of dealing with hanging nodes.

For all $n \in \mathbb{N}$, with each $\mathcal{T}_n$, we associate $\mathcal{E}_n$, $\mathcal{E}_n^I$ and $\mathcal{E}_n^B$, which denote its set of edges, internal edges and boundary edges, respectively. Moreover, with each element K of $\mathcal{T}_n$, we associate $\mathcal{E}^K$, the set of its edges. Finally, we set for all $K \in \mathcal{T}_n$ and for all $n \in \mathbb{N}$,

$$h_K := \text{diam}(K), \quad h := \max_{K\in\mathcal{T}_n} h_K, \quad h_e := \text{length}(e), \ \forall e \in \mathcal{E}^K,$$

and we denote by $\mathbf{x}_K$ the centroid of K.

We say that $\{\mathcal{T}_n\}_{n\in\mathbb{N}}$ is a *regular sequence of polygonal decompositions* if the following assumptions are satisfied:

(**D1**) there exists a positive constant ρ_1 such that, for all $n \in \mathbb{N}$ and for all $K \in \mathcal{T}_n$, $h_e \geq \rho_1 h_K$ for all edges e of K;

(**D2**) there exists a positive constant ρ_2 such that, for all $n \in \mathbb{N}$ and for all $K \in \mathcal{T}_n$, K is star-shaped with respect to a ball of radius greater than or equal to $\rho_2 h_K$.

The assumptions (**D1**) and (**D2**) imply the following property:

(**D3**) there exists a constant $\Lambda \in \mathbb{N}$ such that, for all $n \in \mathbb{N}$ and for all $K \in \mathcal{T}_n$, card($\mathcal{E}^K$)$\leq \Lambda$, that is, the number of edges of each element is uniformly bounded.

We point out that, in this definition, we are not requiring any quasi-uniformity on the size of the elements. A discussion of VEM under more general mesh assumptions is the topic of [20,29].

Remark 1 In the forthcoming analysis, we will employ a number of standard functional inequalities (such as the Poincaré inequality and trace inequalities). It can be proven that the constants appearing in such inequalities depend solely on the parameters ρ_1, ρ_2, and Λ introduced in (**D1**)–(**D3**). We will omit such a dependence, for ease of notation.

For future use, we also define local bilinear forms on polygons $K \in \mathcal{T}_n$ as

$$a^K(u, v) := (\nabla u, \nabla v)_{0,K} \quad \forall u, v \in H^1(K). \tag{4}$$

2.3 Non-conforming Sobolev Spaces

Having introduced the concept of regular sequences of meshes, we pinpoint the concept of sequences of broken and non-conforming Sobolev spaces, along with their norms. For all $n \in \mathbb{N}$ and $s > 0$, we define the broken Sobolev spaces on $\mathcal{T}_n$ as

$$H^s(\mathcal{T}_n) := \left\{ v \in L^2(\Omega) \mid v_{|_K} \in H^s(K)\ \forall K \in \mathcal{T}_n \right\}$$

and the corresponding broken seminorms and norms

$$|v|^2_{s,\mathcal{T}_n} := \sum_{K \in \mathcal{T}_n} |v|^2_{s,K}, \quad \|v\|^2_{s,\mathcal{T}_n} := \sum_{K \in \mathcal{T}_n} \|v\|^2_{s,K}. \tag{5}$$

Particular emphasis is stressed on the broken H^1 bilinear form

$$(u, v)_{1,\mathcal{T}_n} := \sum_{K \in \mathcal{T}_n} (\nabla u, \nabla v)_{0,K}.$$

In order to define non-conforming Sobolev spaces associated with polygonal decompositions, we need to fix some additional notation. In particular, given any internal edge $e \in \mathcal{E}_n^I$ shared by the polygons K^- and K^+ in $\mathcal{T}_n$, we denote by $\mathbf{n}^e_{K^\pm}$ the two outer normal unit vectors with respect to $K^\pm$. For simplicity, we will later only write $\mathbf{n}_{K^\pm}$ instead of $\mathbf{n}^e_{K^\pm}$. Moreover, for boundary edges $e \in \mathcal{E}_n^B$, we introduce the normal unit vector $\mathbf{n}_\Omega$ pointing outside Ω. Having this, for any $v \in H^1(\mathcal{T}_n)$, we set the jump operator across an edge $e \in \mathcal{E}_n$ to

$$[\![v]\!] := \begin{cases} v_{|_{K^+}} \mathbf{n}_{K^+} + v_{|_{K^-}} \mathbf{n}_{K^-} & \text{if } e \in \mathcal{E}_n^I \\ v\mathbf{n}_\Omega & \text{if } e \in \mathcal{E}_n^B. \end{cases} \tag{6}$$

Finally, we introduce the global non-conforming Sobolev space of order $k \in \mathbb{N}$ with respect to the decomposition $\mathcal{T}_n$ incorporating boundary conditions in a *non-conforming sense*: Given $g \in H^{1/2}(\partial\Omega)$ and $k \in \mathbb{N}$, we define

$$\begin{aligned} H_g^{1,nc}(\mathcal{T}_n, k) := \{ v \in H^1(\mathcal{T}_n) \mid & \int_e [\![v]\!] \cdot \mathbf{n}\, q_{k-1}\, \mathrm{d}s = 0 \quad \forall q_{k-1} \in \mathbb{P}_{k-1}(e),\ \forall e \in \mathcal{E}_n^I, \\ & \int_e [\![v]\!] \cdot \mathbf{n}\, q_{k-1}\, \mathrm{d}s = \int_e g q_{k-1}\, \mathrm{d}s \quad \forall q_{k-1} \in \mathbb{P}_{k-1}(e),\ \forall e \in \mathcal{E}_n^B \}, \end{aligned} \tag{7}$$

where $\mathbf{n}$ is either of the two normal unit vectors to e, but fixed, if $e \in \mathcal{E}_n^I$, and $\mathbf{n} = \mathbf{n}_\Omega$, if $e \in \mathcal{E}_n^B$. In the homogeneous case, definition (7) becomes

$$H_0^{1,nc}(\mathcal{T}_n, k) := \left\{ v \in H^1(\mathcal{T}_n) \mid \int_e [\![v]\!] \cdot \mathbf{n}\, q_{k-1}\, \mathrm{d}s = 0 \quad \forall q_{k-1} \in \mathbb{P}_{k-1}(e),\ \forall e \in \mathcal{E}_n \right\}. \tag{8}$$

Importantly, the seminorm $|\cdot|_{1,\mathcal{T}_n}$ is actually a norm for functions in $H_0^{1,nc}(\mathcal{T}_n, k)$. In [28], the validity of the following Poincaré inequality was proven: there exists a positive constant c_P only depending on Ω such that, for all $k \in \mathbb{N}$,

$$\|v\|_{0,\Omega} \leq c_P |v|_{1,\mathcal{T}_n} \quad \forall v \in H_0^{1,nc}(\mathcal{T}_n, k). \tag{9}$$

3 Non-conforming Harmonic Virtual Element Methods

In this section, we introduce a non-conforming harmonic virtual element method for the approximation of problem (2) and investigate its h- and p-versions. To this purpose, in addition to (**D1**)–(**D3**), we will also require on the sequence of meshes $\{\mathcal{T}_n\}_{n\in\mathbb{N}}$ the following quasi-uniformity assumption:

(**D4**) there exists a constant $\rho_3 \geq 1$ such that, for all $n \in \mathbb{N}$ and for all K_1 and K_2 in $\mathcal{T}_n$, it holds $h_{K_2} \leq \rho_3 h_{K_1}$.

We want to approximate problem (2) with a method of the following type:

$$\begin{cases} \text{find } u_n \in V_{n,g}^{\Delta,p} \text{ such that} \\ a_n(u_n, v_n) = 0 \quad \forall v_n \in V_{n,0}^{\Delta,p}, \end{cases} \tag{10}$$

where the space of trial functions $V_{n,g}^{\Delta,p}$ and the space of test functions $V_{n,0}^{\Delta,p}$ are finite dimensional (non-conforming) spaces on a mesh $\mathcal{T}_n$, "mimicking" the infinite dimensional spaces V_g and V_0, defined in (3), respectively. Moreover, $a_n(\cdot,\cdot) : V_{n,g}^{\Delta,p} \times V_{n,0}^{\Delta,p} \to \mathbb{R}$ is a *computable* discrete bilinear form mimicking its continuous counterpart defined again in (3). Such approximation spaces and discrete bilinear forms have to be tailored so that method (10) is well-posed and provides "good" h- and p-approximation estimates.

The outline of this section is as follows. We first introduce suitable global approximation spaces $V_{n,g}^{\Delta,p}$ and $V_{n,0}^{\Delta,p}$ in Sect. 3.1, highlighting their approximation properties in Sect. 3.2. Next, in Sect. 3.3, we define and provide an *explicit* discrete bilinear form and, moreover, we discuss its properties. An abstract error analysis is carried out in Sect. 3.4; such analysis is instrumental for the h- and p-error estimates proved in Sect. 3.5. L^2 error bounds are provided in Sect. 3.6. Finally, in Sect. 3.7, we give a hint concerning the extension to the 3D case and we stress the main differences between the 2D and 3D cases. Some details on the implementation of the method are presented in "Appendix A".

3.1 Non-conforming Harmonic Virtual Element Spaces

The aim of the present section is to introduce non-conforming harmonic virtual element spaces with *uniform* degree of accuracy. To this purpose, we begin with the description of the local harmonic VE spaces, modifying those in [36] into a new setting suited for building global non-conforming spaces.

Let $p \in \mathbb{N}$ be a given parameter. For all $n \in \mathbb{N}$ and for all $K \in \mathcal{T}_n$, we set

$$V^{\Delta}(K) := \left\{ v_n \in H^1(K) \mid \Delta v_n = 0 \text{ in } K,\ (\nabla v_n \cdot \mathbf{n}_K)_{|e} \in \mathbb{P}_{p-1}(e)\ \forall e \in \mathcal{E}^K \right\}. \tag{11}$$

In words, $V^{\Delta}(K)$ consists of *harmonic* functions with piecewise (discontinuous) polynomial normal traces on the boundary of K.

The space $V^{\Delta}(K)$ has dimension $N_K p$, N_K being the number of edges of K. A set of $N_K p$ degrees of freedom for $V^{\Delta}(K)$ is the following. Given $v_n \in V^{\Delta}(K)$,

$$\frac{1}{h_e}\int_e v_n m_r^e \,\mathrm{d}s \quad \forall r = 0, \ldots, p-1,\ \forall e \in \mathcal{E}^K, \tag{12}$$

where $\{m_r^e\}_{r=0,\ldots,p-1}$ is *any* basis of $\mathbb{P}_{p-1}(e)$. These degrees of freedom are in fact unisolvent since, if $v_n \in V^{\Delta}(K)$ has all the degrees of freedom equal to 0, then

$$|\nabla v_n|_{1,K}^2 = \int_K \underbrace{(-\Delta v_n)}_{=0} v_n \,\mathrm{d}x + \int_{\partial K} (\nabla v_n \cdot \mathbf{n}_K)\, v_n \,\mathrm{d}s = \sum_{e\in\mathcal{E}^K} \int_e \underbrace{(\nabla v_n \cdot \mathbf{n}_K)}_{\in\mathbb{P}_{p-1}(e)} v_n \,\mathrm{d}s = 0,$$

which implies that v_n is constant. This, in addition to

$$h_e v_n = \int_e v_n \,\mathrm{d}s = \int_e 1\, v_n \,\mathrm{d}s = 0,$$

for some edge $e \in \mathcal{E}^K$, implies $v_n = 0$, providing unisolvence.

We denote by $\{\varphi_{j,r}\}_{\substack{j=1\dots,N_K \\ r=0,\dots,p-1}}$ the local canonical basis associated with the set of degrees of freedom (12), namely

$$\mathrm{dof}_{i,s}\left(\varphi_{j,r}\right) = \begin{cases} 1 & \text{if } i = j \text{ and } s = r \\ 0 & \text{otherwise} \end{cases} \quad \forall\, i, j = 1, \dots, N_K,\ \forall\, s, r = 0, \dots, p-1. \tag{13}$$

We underline that the indices i and j refer to the edge, whereas the indices s and r refer to the polynomial m_r^e employed in the definition of the local degrees of freedom (12).

It is worth to note that the local canonical basis consists of functions that are not explicitly known inside the element and even their polynomial normal traces over the boundary are unknown.

By employing the degrees of freedom defined in (12), it is possible to compute the following two projectors. The first one is the edge L^2 projector onto the space of polynomials of degree $p-1$

$$\begin{aligned} &\Pi^{0,e}_{p-1} : V^{\Delta}(K)|_e \to \mathbb{P}_{p-1}(e), \\ &\int_e \left(v_n - \Pi^{0,e}_{p-1} v_n\right) q^e_{p-1}\,\mathrm{d}s = 0 \quad \forall v_n \in V^{\Delta}(K),\ \forall q^e_{p-1} \in \mathbb{P}_{p-1}(e). \end{aligned} \tag{14}$$

The second one is the bulk H^1 projector onto the space of harmonic polynomials of degree p

$$\begin{aligned} &\Pi^{\nabla,\Delta,K}_p = \Pi^{\nabla,K}_p : V^{\Delta}(K) \to \mathbb{H}_p(K), \\ &\int_K \nabla\left(v_n - \Pi^{\nabla,K}_p v_n\right)\cdot \nabla q^{\Delta}_p \,\mathrm{d}x = 0 \quad \forall v_n \in V^{\Delta}(K),\ \forall q^{\Delta}_p \in \mathbb{H}_p(K), \\ &\int_{\partial K} \left(v_n - \Pi^{\nabla,K}_p v_n\right) \mathrm{d}s = 0 \quad \forall v_n \in V^{\Delta}(K), \end{aligned} \tag{15}$$

where the last condition is imposed in order to define the projector in a unique way.

We are ready to define global non-conforming harmonic VE spaces, which incorporate Dirichlet boundary conditions in a "non-conforming sense". Let $p \in \mathbb{N}$ be a given parameter. Then, for any $g \in H^{1/2}(\partial\Omega)$, we set

$$V^{\Delta,p}_{n,g} := \left\{ v_n \in H^{1,nc}_g(\mathcal{T}_n, p) \ \middle|\ v_{n|K} \in V^{\Delta}(K)\ \forall K \in \mathcal{T}_n \right\}. \tag{16}$$

We observe the following facts:

- Definition (16) includes the space of test functions $V^{\Delta,p}_{n,0}$, by selecting $g = 0$.
- The parameter p in (16) indicates the level of non-conformity of the method. The fact that the non-conformity is defined with respect to Dirichlet traces allows us to easily couple the local degrees of freedom into a global set, provided that we choose the same value p for the non-conformity parameter and for the polynomial degree entering definition (11) of the local spaces. The resulting global set of degrees of freedom is of dimension $\mathrm{card}(\mathcal{E}_n)\,p$.
- Dirichlet boundary conditions on $\partial\Omega$ are imposed weakly via the definition of the non-conforming spaces (7) and (8). For instance, given a Dirichlet datum g, on all boundary

edges $e \in \mathcal{E}_n^B$, we set

$$\int_e [\![v_n]\!] \cdot \mathbf{n}_\Omega \, q_{p-1}^e \, \mathrm{d}s = \int_e v_n q_{p-1}^e \, \mathrm{d}s = \int_e g q_{p-1}^e \, \mathrm{d}s \quad \forall v_n \in V_{n,g}^{\Delta,p}, \ \forall q_{p-1}^e \in \mathbb{P}_{p-1}(e).$$

Remark 2 We highlight that, at the discrete level, one should also take into account the approximation of the Dirichlet boundary condition g. In practice, assuming $g \in H^{\frac{1}{2}+\varepsilon}(\partial\Omega)$, for any $\varepsilon > 0$ arbitrarily small, and denoting by g_p the approximation of g obtained by interpolating g at the $p+1$ Gauß–Lobatto nodes on each edge in $\mathcal{E}_n^B$, one should define the trial space as

$$V_{n,g}^{\Delta,p} := \left\{ v_n \in H_{g_p}^{1,nc}(\mathcal{T}_n, p) \mid v_{n|_K} \in V^\Delta(K) \, \forall K \in \mathcal{T}_n \right\}.$$

With this definition, in the forthcoming analysis (see Propositions 3.1, 3.8, Theorems 3.3, 3.6, and 3.9 below), an additional term related to the approximation of the Dirichlet datum via Gauß–Lobatto interpolants should be taken into account. However, following [26, Theorems 4.2, 4.5], it is possible to show that the h- and p-rates of convergence of the method are not spoilt by this term. For this reason and for the sake of simplicity, we will neglect in the following the presence of this term and assume that the approximation space is the one defined in (16).

3.2 Approximation Properties of Functions in Non-conforming Harmonic Virtual Element Spaces

In this section, we deal with approximation properties of functions in the non-conforming harmonic VE spaces $V_{n,g}^{\Delta,p}$ and $V_{n,0}^{\Delta,p}$.

Since h- and p-approximation properties of harmonic functions via harmonic polynomials are known, see e.g. [11,45], we want to relate best approximation estimates in the non-conforming harmonic VE spaces to the corresponding ones in *discontinuous* harmonic polynomial spaces. In particular, we prove the following result.

Proposition 3.1 *Given $g \in H^{1/2}(\partial\Omega)$, let $u \in V_g$, where V_g is defined in (3). For any polygonal partition $\mathcal{T}_n$ of Ω, there exists $u_I \in V_{n,g}^{\Delta,p}$, with $V_{n,g}^{\Delta,p}$ introduced in (16), such that*

$$|u - u_I|_{1,\mathcal{T}_n} \leq 2 \left| u - q_p^\Delta \right|_{1,\mathcal{T}_n} \quad \forall q_p^\Delta \in \mathcal{S}^{p,\Delta,-1}(\mathcal{T}_n),$$

where $\mathcal{S}^{p,\Delta,-1}(\mathcal{T}_n)$ is the space of discontinuous piecewise harmonic polynomials of degree at most p, that is,

$$\mathcal{S}^{p,\Delta,-1}(\mathcal{T}_n) := \left\{ q \in L^2(\Omega) : q_{|_K} \in \mathbb{H}_p(K) \, \forall K \in \mathcal{T}_n \right\}. \tag{17}$$

Proof Define $u_I \in V_{n,g}^{\Delta,p}$ by

$$\int_e (u - u_I) q_{p-1}^e \, \mathrm{d}s = 0 \quad \forall q_{p-1}^e \in \mathbb{P}_{p-1}(e), \ \forall e \in \mathcal{E}_n, \tag{18}$$

that is, we fix the degrees of freedom (12) of u_I to be equal to the values of the same functionals applied to the solution u. Having this, it holds

$$|u - u_I|_{1,\mathcal{T}_n} \leq \left| u - q_p^\Delta \right|_{1,\mathcal{T}_n} + \left| u_I - q_p^\Delta \right|_{1,\mathcal{T}_n} \quad \forall q_p^\Delta \in \mathcal{S}^{p,\Delta,-1}(\mathcal{T}_n), \tag{19}$$

where $\mathcal{S}^{p,\Delta,-1}(\mathcal{T}_n)$ is defined in (17). We focus on the second term on the right-hand side of (19). By integrating by parts and using (18), together with the definition of the space (16), we get

$$\begin{aligned}
\left|u_I - q_p^\Delta\right|_{1,\mathcal{T}_n}^2 &= \sum_{K\in\mathcal{T}_n} \left|u_I - q_p^\Delta\right|_{1,K}^2 \\
&= \sum_{K\in\mathcal{T}_n} \left\{ \int_K \left(u_I - q_p^\Delta\right) \left(\underbrace{-\Delta\left(u_I - q_p^\Delta\right)}_{=0} \right) \mathrm{d}x + \sum_{e\in\mathcal{E}^K} \int_e \left(u_I - q_p^\Delta\right) \nabla\left(u_I - q_p^\Delta\right)\cdot \mathbf{n}_K \,\mathrm{d}s \right\} \quad (20)\\
&= \sum_{K\in\mathcal{T}_n} \sum_{e\in\mathcal{E}^K} \int_e \left(u - q_p^\Delta\right) \nabla\left(u_I - q_p^\Delta\right)\cdot \mathbf{n}_K \,\mathrm{d}s.
\end{aligned}$$

By expanding the right-hand side of (20) and using the Cauchy–Schwarz inequality, we obtain

$$\begin{aligned}
\left|u_I - q_p^\Delta\right|_{1,\mathcal{T}_n}^2 &= \sum_{K\in\mathcal{T}_n} \int_K \nabla\left(u - q_p^\Delta\right)\cdot\nabla\left(u_I - q_p^\Delta\right)\mathrm{d}x + \int_K \left(u - q_p^\Delta\right) \underbrace{\Delta\left(u_I - q_p^\Delta\right)}_{=0} \mathrm{d}x \\
&\le \left|u - q_p^\Delta\right|_{1,\mathcal{T}_n} \left|u_I - q_p^\Delta\right|_{1,\mathcal{T}_n}.
\end{aligned}$$

Inserting this into (19) gives the result. □

We remark that, with a similar proof of that of Proposition 3.1, one can prove an equivalent result for the non-conforming (non-harmonic) VE spaces of [7]; see Proposition 3.8 below.

3.3 Discrete Bilinear Forms

In this section, we complete the definition of the method (10) by introducing a suitable bilinear form $a_n(\cdot,\cdot)$, which is explicitly computable. We follow here the typical VEM gospel [13,18,36]. It is important to highlight that the local bilinear forms $a^K(\cdot,\cdot)$ defined in (4) are not explicitly computable on the whole discrete spaces since an explicit representation of functions in the harmonic VE spaces is not available in closed form.

Therefore, we aim at introducing explicit computable discrete bilinear forms $a_n^K(\cdot,\cdot)$ which mimic their continuous counterparts $a^K(\cdot,\cdot)$. To this purpose, we observe that the Pythagorean theorem yields

$$\begin{aligned}
&a^K(u_n, v_n) = a^K\left(\Pi_p^{\nabla,K} u_n, \Pi_p^{\nabla,K} v_n\right) + a^K\left(\left(I - \Pi_p^{\nabla,K}\right)u_n, \left(I - \Pi_p^{\nabla,K}\right)v_n\right) \\
&\quad \forall u_n,\ v_n \in V^\Delta(K),
\end{aligned} \quad (21)$$

where we recall that $\Pi_p^{\nabla,K}$ is defined in (15). The first term on the right-hand side of (21) is computable, whereas the second is not. Thus, following [36] and the references therein, we replace this term by a *computable* symmetric bilinear form $S^K : \ker(\Pi_p^{\nabla,K}) \times \ker(\Pi_p^{\nabla,K}) \to \mathbb{R}$, such that

$$c_*(p)|v_n|_{1,K}^2 \le S^K(v_n, v_n) \le c^*(p)|v_n|_{1,K}^2 \quad \forall v_n \in \ker\left(\Pi_p^{\nabla,K}\right), \quad (22)$$

where $c_*(p)$ and $c^*(p)$ are two positive constants which may depend on p, but are independent of K and, in particular, of h_K.

Hence, depending on the choice of the stabilization, a class of candidates for the local discrete symmetric bilinear forms is

$$a_n^K(u_n, v_n) = a^K\left(\Pi_p^{\nabla,K} u_n, \Pi_p^{\nabla,K} v_n\right) + S^K\left(\left(I - \Pi_p^{\nabla,K}\right) u_n, \left(I - \Pi_p^{\nabla,K}\right) v_n\right) \quad \forall u_n,\ v_n \in V^\Delta(K). \tag{23}$$

The forms $a_n^K(\cdot,\cdot)$ satisfy the two following properties:

(**P1**) p-**harmonic consistency**: for all $K \in \mathcal{T}_n$ and for all $p \in \mathbb{N}$,

$$a^K\left(q_p^\Delta, v_n\right) = a_n^K\left(q_p^\Delta, v_n\right) \quad \forall q_p^\Delta \in \mathbb{H}_p(K),\ \forall v_n \in V^\Delta(K); \tag{24}$$

(**P2**) **stability**: for all $K \in \mathcal{T}_n$ and for all $p \in \mathbb{N}$,

$$\alpha_*(p)|v_n|_{1,K}^2 \leq a_n^K(v_n, v_n) \leq \alpha^*(p)|v_n|_{1,K}^2 \quad \forall v_n \in V^\Delta(K), \tag{25}$$

where $\alpha_*(p) = \min(1, c_*(p))$ and $\alpha^*(p) = \max(1, c^*(p))$.

Owing to property (**P1**), p can be addressed to as *degree of accuracy of the method*, since whenever either of its two entries is a harmonic polynomial of degree p, the local discrete bilinear form can be computed exactly, up to machine precision. Moreover, since $a_n^K(\cdot,\cdot)$ is assumed to be symmetric, (**P2**) implies continuity

$$a_n^K(u_n, v_n) \leq \left(a_n^K(u_n, u_n)\right)^{1/2}\left(a_n^K(v_n, v_n)\right)^{1/2} \leq \alpha^*(p)|u_n|_{1,K}|v_n|_{1,K} \quad \forall u_n, v_n \in V^\Delta(K). \tag{26}$$

The global discrete bilinear form is defined as

$$a_n(u_n, v_n) = \sum_{K\in\mathcal{T}_n} a_n^K(u_n, v_n) \quad \forall u_n \in V_{n,g_1}^{\Delta,p},\ \forall v_n \in V_{n,g_2}^{\Delta,p} \tag{27}$$

for all $g_1, g_2 \in H^{1/2}(\partial\Omega)$. The remainder of this section is devoted to introduce an explicit stabilization $S^K(\cdot,\cdot)$ with explicit bounds of the constants $c_*(p)$ and $c^*(p)$.

For all $K \in \mathcal{T}_n$, we define

$$S^K(u_n, v_n) = \sum_{e\in\mathcal{E}^K} \frac{p}{h_e}\left(\Pi_{p-1}^{0,e} u_n, \Pi_{p-1}^{0,e} v_n\right)_{0,e} \quad \forall u_n,\ v_n \in \ker\left(\Pi_p^{\nabla,K}\right). \tag{28}$$

For this choice of stabilization forms, the following result holds true.

Theorem 3.2 *Assume that (**D1**) and (**D2**) hold true. Then, for any $K \in \mathcal{T}_n$, the stabilization $S^K(\cdot,\cdot)$ defined in (28) satisfies (22) with the bounds*

$$c_*(p) \gtrsim p^{-2}, \quad c^*(p) \lesssim \begin{cases} p\left(\frac{\log(p)}{p}\right)^{\frac{\lambda_K}{2}} & \text{if } K \text{ is convex} \\ p\left(\frac{\log(p)}{p}\right)^{\frac{\lambda_K}{2\omega_K}-\varepsilon} & \text{otherwise} \end{cases} \tag{29}$$

for all $\varepsilon > 0$ arbitrarily small, where the hidden constants in (29) are independent of h and p, and where $\omega_K\pi$ and $\lambda_K\pi$, with ω_K and $\lambda_K \in (0, 2)$, denote the largest interior and the smallest exterior angles of K, respectively.

Proof We assume, without loss of generality, that $h_K = 1$; the general result follows from a scaling argument.

For any function v_n in $V^{\Delta}(K)$, we have

$$
\begin{aligned}
|v_n|^2_{1,K} &= -\int_K \underbrace{(\Delta v_n)}_{=0} v_n \,\mathrm{d}x + \int_{\partial K} \nabla v_n \cdot \mathbf{n}_K \, v_n \,\mathrm{d}s \\
&= \sum_{e\in\mathcal{E}^K} \int_e \nabla v_n \cdot \mathbf{n}_K \left(\Pi^{0,e}_{p-1} v_n\right) \mathrm{d}s \le \|\nabla v_n \cdot \mathbf{n}_K\|_{0,\partial K} \left\|\Pi^{0,\partial K}_{p-1} v_n\right\|_{0,\partial K}
\end{aligned}
\tag{30}
$$

where we have set, with an abuse of notation, $(\Pi^{0,\partial K}_{p-1} v_n)_{|e} = \Pi^{0,e}_{p-1}(v_{n|e})$.We prove that

$$
\|\nabla v_n \cdot \mathbf{n}_K\|_{0,\partial K} \lesssim p^{\frac{3}{2}} \|\nabla v_n \cdot \mathbf{n}_K\|_{-\frac{1}{2},\partial K}. \tag{31}
$$

To this end, we set, for the sake of simplicity, $r_p := \nabla v_n \cdot \mathbf{n}_K$, and consider the case $r_p \neq 0$. One has $r_p \in L^2(\partial K)$ with $r_{p|e} \in \mathbb{P}_p(e)$ for all $e \in \mathcal{E}^K$. In general, $r_p \notin H^{1/2}(\partial K)$. Further, we introduce the piecewise bubble function $b_{\partial K} \in H^{1/2}(\partial K)$ defined edgewise as

$$
(b_{\partial K})_{|e}(\mathbf{x}) := \left(\beta \circ \phi_e^{-1}\right)(\mathbf{x}) \quad \forall e \in \mathcal{E}^K,
$$

where $\phi_e : [-1, 1] \to e$ is the linear transformation mapping the interval $[-1, 1]$ to the edge e, and $\beta : [-1, 1] \to [0, 1]$ is the 1D quadratic bubble function $\beta(x) := 4(1 - x^2)$.

From the definition of the $H^{-1/2}(\partial K)$ norm, the fact that $r_p \in L^2(\partial K)$, and $r_p b_{\partial K} \in H^{1/2}(\partial K)\backslash\{0\}$, we have

$$
\|r_p\|_{-\frac{1}{2},\partial K} = \sup_{\psi\in H^{1/2}(\partial K)\backslash\{0\}} \frac{(r_p,\psi)_{0,\partial K}}{\|\psi\|_{\frac{1}{2},\partial K}} \ge \frac{(r_p, r_p b_{\partial K})_{0,\partial K}}{\left\|r_p b_{\partial K}\right\|_{\frac{1}{2},\partial K}} = \frac{\left\|r_p b^{\frac{1}{2}}_{\partial K}\right\|^2_{0,\partial K}}{\left\|r_p b_{\partial K}\right\|_{\frac{1}{2},\partial K}}. \tag{32}
$$

We have the two following polynomial p-inverse inequalities:

$$
\left\|r_p b_{\partial K}\right\|_{0,e} \le \left\|r_p b^{\frac{1}{2}}_{\partial K}\right\|_{0,e}, \quad \left|r_p b_{\partial K}\right|_{1,e} \lesssim p \left\|r_p b^{\frac{1}{2}}_{\partial K}\right\|_{0,e} \quad \forall e \in \mathcal{E}^K. \tag{33}
$$

The first one is a direct consequence of the fact that the range of $b_{\partial K}$ is [0, 1], and the second one follows from [12, Lemma 2]. Using (33), summing over all edges $e \in \mathcal{E}^K$, and applying interpolation theory, lead to

$$
\left\|r_p b_{\partial K}\right\|_{\frac{1}{2},\partial K} \lesssim p^{\frac{1}{2}} \left\|r_p b^{\frac{1}{2}}_{\partial K}\right\|_{0,\partial K},
$$

which, together with (32), gives

$$
\|r_p\|_{-\frac{1}{2},\partial K} \gtrsim p^{-\frac{1}{2}} \left\|r_p b^{\frac{1}{2}}_{\partial K}\right\|_{0,\partial K} \gtrsim p^{-\frac{3}{2}} \left\|r_p\right\|_{0,\partial K},
$$

where in the last inequality, [25, Lemma 4] was used. The bound (31) follows immediately.

From (30) and (31), taking also into account that $\Delta v_n = 0$ in K, we get

$$
|v_n|^2_{1,K} \lesssim p^{\frac{3}{2}} \|\nabla v_n \cdot \mathbf{n}_K\|_{-\frac{1}{2},\partial K} \left\|\Pi^{0,\partial K}_{p-1} v_n\right\|_{0,\partial K} \lesssim p^{\frac{3}{2}} |v_n|_{1,K} \left\|\Pi^{0,\partial K}_{p-1} v_n\right\|_{0,\partial K},
$$

where in the last step we have used a Neumann trace inequality, see e.g. [56, Theorem A.33]. This proves the first inequality of (22) with $c_*(p) \gtrsim p^{-2}$.

In order to prove the second one, we can write

$$\left\| \Pi^{0,\partial K}_{p-1} v_n \right\|_{0,\partial K} \leq \|v_n\|_{0,\partial K} \lesssim \|v_n\|^{\frac{1}{2}}_{0,K} \, |v_n|^{\frac{1}{2}}_{1,K} \,, \tag{34}$$

where we have used the stability of the L^2 projection, the multiplicative trace inequality, and the Poincaré inequality, see [28], which is valid since $v_n \in \ker(\Pi^{\nabla,K}_p)$ and thus has zero mean value on ∂K, see (15).

Let us bound the first factor on the right-hand side of (34). To this end, we define $\overline{v}_n$ as the average of v_n over the polygon K. A triangle inequality yields

$$\|v_n\|_{0,K} \leq \|v_n - \overline{v}_n\|_{0,K} + \|\overline{v}_n\|_{0,K}. \tag{35}$$

Recalling that v_n has zero average over ∂K, we have

$$\|\overline{v}_n\|_{0,K} = |K|^{\frac{1}{2}} |\overline{v}_n| = \frac{|K|^{\frac{1}{2}}}{|\partial K|} \left| \int_{\partial K} \overline{v}_n - v_n \, \mathrm{d}s \right|.$$

A Cauchy–Schwarz inequality, together with the multiplicative trace inequality, yields

$$\|\overline{v}_n\|_{0,K} \lesssim \|v_n - \overline{v}_n\|^{\frac{1}{2}}_{0,K} |v_n|^{\frac{1}{2}}_{1,K}.$$

Inserting this inequality in (35) gives

$$\|v_n\|_{0,K} \lesssim \|v_n - \overline{v}_n\|_{0,K} + \|v_n - \overline{v}_n\|^{\frac{1}{2}}_{0,K} |v_n|^{\frac{1}{2}}_{1,K}. \tag{36}$$

From [36, Lemma 3.2], we have

$$\|v_n - \overline{v}_n\|^{\frac{1}{2}}_{0,K} \lesssim \begin{cases} \left(\frac{\log(p)}{p}\right)^{\lambda_K} |v_n|_{1,K} & \text{if } K \text{ is convex} \\ \left(\frac{\log(p)}{p}\right)^{\frac{\lambda_K}{\omega_K} - \varepsilon} |v_n|_{1,K} & \text{otherwise} \end{cases}$$

for all $\varepsilon > 0$ arbitrarily small. Inserting this into (36) gives

$$\|v_n\|_{0,K} \lesssim \begin{cases} \left(\frac{\log(p)}{p}\right)^{\frac{\lambda_K}{2}} |v_n|_{1,K} & \text{if } K \text{ is convex} \\ \left(\frac{\log(p)}{p}\right)^{\frac{\lambda_K}{2\omega_K} - \varepsilon} |v_n|_{1,K} & \text{otherwise,} \end{cases}$$

which, together with (34), gives (22) with $c^*(p)$ as in (29). □

Owing to (25) and (29) one deduces

$$\alpha_*(p) \gtrsim p^{-2}, \quad \alpha^*(p) \lesssim \begin{cases} p \left(\frac{\log(p)}{p}\right)^{\frac{\lambda_K}{2}} & \text{if } K \text{ is convex} \\ p \left(\frac{\log(p)}{p}\right)^{\frac{\lambda_K}{2\omega_K} - \varepsilon} & \text{otherwise} \end{cases}$$

for all $\varepsilon > 0$ arbitrarily small.

Remark 3 In the conforming harmonic VEM setting [36], the following local stabilization forms were introduced:

$$S^K(u_n, v_n) = (u_n, v_n)_{\frac{1}{2},\partial K} \quad \forall K \in \mathcal{T}_n.$$

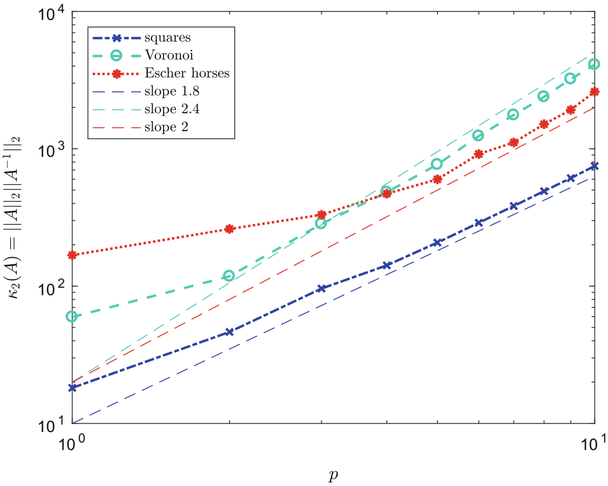

Fig. 1 Condition number for different values of p of the global stiffness matrix obtained with the local stabilization forms in (28). A Cartesian mesh, a Voronoi-Lloyd mesh, and an Escher horses mesh have been considered. We observe algebraic growth of the condition number with p for all the tested meshes

It was proven that employing such stabilization forms leads to have stability constants $\alpha_*(p)$ and $\alpha^*(p)$ that are independent of the degree of accuracy p. However, in the present nonconforming setting, such a stabilization is not computable, as the Dirichlet traces of functions in the local VE spaces are not available in closed form.

We investigate numerically the behavior of the conditioning of the global VE matrix in terms of the degree of accuracy p, when employing the local stabilization forms in (28). In Fig. 1, we plot the condition number for different values of p, when computing the global stiffness matrix on a Cartesian mesh, a Voronoi-Lloyd mesh , and an Escher horses mesh, see Fig. 2, and note that it grows algebraically with p. We remark that the condition number of standard (non-harmonic) VEM can grow exponentially or algebraically with p, depending on the choice of the internal degrees of freedom. This was investigated in [48].

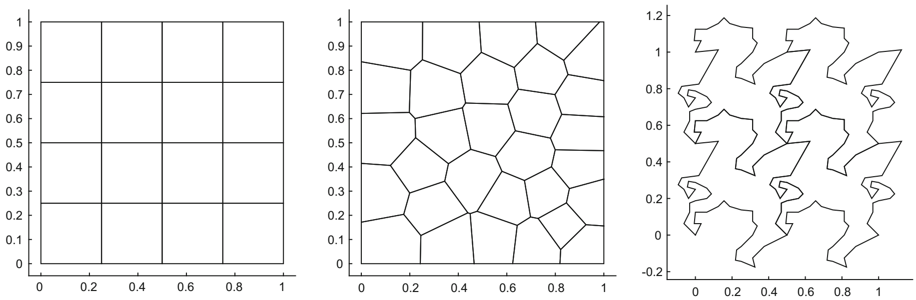

Fig. 2 Different types of meshes: mesh made of squares (left), Voronoi-Llyod mesh (center), and mesh made of Escher horses (right)

3.4 Abstract Error Analysis

Along the lines of [13,17,36], we provide in this section an abstract error analysis of the method (10), taking into account the non-conformity of the approximation. To this purpose, we introduce the auxiliary bilinear form

$$\mathcal{N}_n : H^1(\Omega) \times H_0^{1,nc}(\mathcal{T}_n, p) \to \mathbb{R}, \quad \mathcal{N}_n(u, v) = \sum_{e \in \mathcal{E}_n} \int_e \nabla u \cdot [\![v]\!] \, \mathrm{d}s. \tag{37}$$

The following convergence result holds true.

Theorem 3.3 *Assume that (**D1**) and (**D2**) hold true and consider the non-conforming harmonic VEM (10) defined by choosing the harmonic VE spaces as in (16) and (11), with level of non-conformity, as well as degree of accuracy, equal to p, and by choosing the discrete bilinear form as in (27) and (23), with stabilization form $S^K(\cdot,\cdot)$ satisfying (22). Then, the method is well-posed and the following bound holds true:*

$$|u - u_n|_{1,\mathcal{T}_n} \leq \frac{\alpha^*(p)}{\alpha_*(p)} \left\{ 6 \inf_{q_p^\Delta \in \mathcal{S}^{p,\Delta,-1}(\mathcal{T}_n)} \left| u - q_p^\Delta \right|_{1,\mathcal{T}_n} + \sup_{v_n \in V_{n,0}^{\Delta,p}} \frac{\mathcal{N}_n(u, v_n)}{|v_n|_{1,\mathcal{T}_n}} \right\}, \tag{38}$$

where we recall that $\mathcal{S}^{p,\Delta,-1}(\mathcal{T}_n)$ is defined in (17), $\mathcal{N}_n(\cdot,\cdot)$ is given in (37), and the stability constants $\alpha_*(p)$ and $\alpha^*(p)$ are introduced in (25).

Proof The well-posedness of the method follows directly from (9), (25) and the Lax–Milgram lemma.

For the bound (38), we observe that

$$|u - u_n|_{1,\mathcal{T}_n} \leq |u - u_I|_{1,\mathcal{T}_n} + |u_n - u_I|_{1,\mathcal{T}_n} \quad \forall u_I \in V_{n,g}^{\Delta,p}.$$

We estimate the second term on the right-hand side. Set $\delta_n := u_n - u_I$. Since $u_n, u_I \in V_{n,g}^{\Delta,p}$, then $\delta_n \in V_{n,0}^{\Delta,p}$. Therefore, for all $q_p^\Delta \in \mathcal{S}^{p,\Delta,-1}(\mathcal{T}_n)$, using (25), (10) and (24), we have

$$\begin{aligned}
|\delta_n|^2_{1,\mathcal{T}_n} &= \sum_{K \in \mathcal{T}_n} |\delta_n|^2_{1,K} \leq \frac{1}{\alpha_*(p)} \sum_{K \in \mathcal{T}_n} a_n^K(\delta_n, \delta_n) = -\frac{1}{\alpha_*(p)} \sum_{K \in \mathcal{T}_n} a_n^K(u_I, \delta_n) \\
&= -\frac{1}{\alpha_*(p)} \left\{ \sum_{K \in \mathcal{T}_n} \left[a_n^K \left(u_I - q_p^\Delta, \delta_n \right) + a^K \left(q_p^\Delta - u, \delta_n \right) \right] + \sum_{K \in \mathcal{T}_n} a^K(u, \delta_n) \right\}.
\end{aligned}$$

The last term on the right-hand side can be rewritten in the spirit of non-conforming methods. More precisely, we observe that an integration by parts, the fact that $\Delta u = 0$ in every $K \in \mathcal{T}_n$, and the definition (37), yield

$$\sum_{K \in \mathcal{T}_n} a^K(u, \delta_n) = \sum_{K \in \mathcal{T}_n} \int_{\partial K} \nabla u \cdot \mathbf{n}_K \, \delta_n \, \mathrm{d}s = \sum_{e \in \mathcal{E}_n} \int_e \nabla u \cdot [\![\delta_n]\!] \, \mathrm{d}s = \mathcal{N}_n(u, \delta_n).$$

This, together with the stability property (25), the triangle and the Cauchy–Schwarz inequalities, gives

$$|\delta_n|^2_{1,\mathcal{T}_n} \leq \frac{1}{\alpha_*(p)} \left[\left(\alpha^*(p) \left(|u_I - u|_{1,\mathcal{T}_n} + \left| u - q_p^\Delta \right|_{1,\mathcal{T}_n} \right) + \left| q_p^\Delta - u \right|_{1,\mathcal{T}_n} \right) |\delta_n|_{1,\mathcal{T}_n} + \mathcal{N}_n(u, \delta_n) \right].$$

Therefore, using Proposition 3.1 and $\alpha^*(p) \geq 1$, we obtain

$$|\delta_n|_{1,\mathcal{T}_n} \leq \frac{1}{\alpha_*(p)} \left[\alpha^*(p) \left(2 \left| u - q_p^\Delta \right|_{1,\mathcal{T}_n} + \left| u - q_p^\Delta \right|_{1,\mathcal{T}_n} \right) + \left| q_p^\Delta - u \right|_{1,\mathcal{T}_n} + \frac{\mathcal{N}_n(u,\delta_n)}{|\delta_n|_{1,\mathcal{T}_n}} \right]$$
$$\leq \frac{\alpha^*(p)}{\alpha_*(p)} \left[4 \left| u - q_p^\Delta \right|_{1,\mathcal{T}_n} + \frac{\mathcal{N}_n(u,\delta_n)}{|\delta_n|_{1,\mathcal{T}_n}} \right],$$

and bound (38) readily follows. □

We refer to the term $\frac{\alpha^*(p)}{\alpha_*(p)}$ appearing in (38) as *pollution factor*.

Remark 4 It is interesting to note that the counterpart of Theorem 3.3 in the conforming version of the harmonic VEM in [36] states that the error of the method is bounded, up to a constant times the pollution factor $\frac{\alpha^*(p)}{\alpha_*(p)}$, by a best approximation error with respect to piecewise discontinuous harmonic polynomials, plus the best approximation error with respect to functions in the global approximation space. In the non-conforming setting of the present paper, however, the latter term is not present, thanks to Proposition 3.1. The additional term here is related to the non-conformity.

3.5 *h*- and *p*-Error Analysis

This section is devoted to the h- and p-analysis of the method (10) employing non-conforming harmonic VE spaces with degree of non-conformity equal to the degree of accuracy of the method.

For the analysis, we have to discuss how to bound the two terms on the right-hand side of (38) in terms of h and p. The first term, i.e., the best approximation error with respect to discontinuous harmonic polynomials, can be dealt with following [50,51]. In particular, we recall the following result from [50, Theorem 2.9] (see also [51, Chapter II]).

Lemma 3.4 *Under the star-shapedness assumption (**D2**), for a given $K \in \mathcal{T}_n$, we denote by $\lambda_K \pi$, $0 < \lambda_K < 2$, its smallest exterior angle. Then, for every harmonic function u in $H^{s+1}(K)$, $s \geq 0$, there exists a sequence $\{q_p^\Delta\}_{p \in \mathbb{N}}$, with $q_p^\Delta \in \mathbb{H}_p(K)$ for all $p \in \mathbb{N}$ with $p \geq s-1$, such that*

$$\left| u - q_p^\Delta \right|_{1,K} \leq c h_K^s \left(\frac{\log(p)}{p} \right)^{\lambda_K s} \|u\|_{s+1,K}, \tag{39}$$

for some positive constant c depending only on ρ_2.

Remark 5 We underline that the p-version approximation of harmonic functions by means of harmonic polynomials has different rates of convergence than that of generic (non-harmonic) functions by means of full polynomials. In particular, from (39), one deduces that, on convex elements, a better convergence rate is achieved (i.e., harmonic functions can be better approximated by polynomials than generic functions, even by considering harmonic polynomials only), while on non-convex elements, the rate of approximation gets worse (i.e., the best approximation of harmonic functions by full polynomials fails to be achieved with harmonic polynomials).

Next, we have to bound the non-conformity term $\mathcal{N}_n(u, v_n)$ introduced in (37). To this purpose, we use tools of non-conforming methods and hp-analysis.

Firstly, we define Ω_{ext} as an extension of the domain Ω, subordinated to polygonal decompositions. More precisely, let $\widetilde{\mathcal{T}}_n$ be a triangulation of Ω which is given by the union of local triangulations $\widetilde{\mathcal{T}}_n(K)$ over each polygon $K \in \mathcal{T}_n$ ($\widetilde{\mathcal{T}}_n$ is nested in $\mathcal{T}_n$); such local triangulations are obtained by connecting the vertices of K to the center of the ball with respect to which K is star-shaped, see assumption (**D2**). With each triangle $T \in \widetilde{\mathcal{T}}_n$, we associate $Q(T)$, a parallelogram obtained by reflecting T with respect to the midpoint of one of its edges, which is arbitrarily fixed. Then, we set

$$\Omega_{\text{ext}} := \bigcup_{T \in \widetilde{\mathcal{T}}_n} Q(T). \tag{40}$$

Notice that Ω_{ext} could coincide with Ω.

The following lemma provides an upper bound for the non-conformity term $\mathcal{N}_n(u, v_n)$.

Lemma 3.5 *Assume that (**D1**)-(**D4**) are satisfied. Then, for all $s \geq 1$ and for all $u \in H^{s+1}(\Omega_{\text{ext}})$, the following bound holds true:*

$$|\mathcal{N}_n(u, v_n)| \leq c\, d^s \frac{h^{\min(s,p)}}{p^s} \|u\|_{s+1,\Omega_{\text{ext}}} |v_n|_{1,\mathcal{T}_n} \quad \forall v_n \in V_{n,0}^{\Delta,p},$$

where c is a positive constant depending only on ρ_1, ρ_2, ρ_3, and Λ, and d is a positive constant.

Proof Without loss of generality, let us assume that $h = 1$, so that $\rho_3^{-1} \leq h_K \leq 1$ for all $K \in \mathcal{T}_n$, due to the assumption (**D4**); the general assertion follows from a scaling argument.

First, we observe that, for all $v_n \in V_{n,0}^{\Delta,p}$, the definition of non-conforming spaces and basic properties of orthogonal projectors yield

$$\begin{aligned} |\mathcal{N}_n(u, v_n)| &= \left| \sum_{e \in \mathcal{E}_n} \int_e \nabla u \cdot [\![v_n]\!] \, \mathrm{d}s \right| = \left| \sum_{e \in \mathcal{E}_n} \int_e \left(\nabla u - \Pi_{p-1}^{0,e}(\nabla u) \right) \cdot \left([\![v_n]\!] - \Pi_{p-1}^{0,e} [\![v_n]\!] \right) \mathrm{d}s \right| \\ &\leq \sum_{e \in \mathcal{E}_n} \left\| \nabla u - \Pi_{p-1}^{0,e}(\nabla u) \right\|_{0,e} \left\| [\![v_n]\!] - \Pi_{p-1}^{0,e} [\![v_n]\!] \right\|_{0,e}, \end{aligned} \tag{41}$$

where we have denoted by $\Pi_{p-1}^{0,e}$, with an abuse of notation, the L^2 projector onto the vectorial polynomial spaces of degree $p-1$ on e.

In order to estimate the first term on the right-hand side, we proceed as follows. Let us consider $\widetilde{\mathcal{T}}_n$, the union of the local triangulations $\widetilde{\mathcal{T}}_n(K)$ of each $K \in \mathcal{T}_n$ defined as above. The triangulation $\widetilde{\mathcal{T}}_n$ has the property that each $T \in \widetilde{\mathcal{T}}_n$ is star-shaped with respect to a ball of radius greater than or equal to $\rho_4 h_T$, where ρ_4 is a positive constant and h_T is the diameter of the triangle T, see [53]. Let now $e \in \mathcal{E}_n$ be fixed and $K \in \mathcal{T}_n$ be a polygon with $e \in \mathcal{E}^K$. Then,

$$\left\| \nabla u - \Pi_{p-1}^{0,e}(\nabla u) \right\|_{0,e} \leq \left\| \nabla u - \Pi_{p-1}^{0,T}(\nabla u) \right\|_{0,e},$$

where $\Pi_{p-1}^{0,T}$ is the L^2 projector onto the space of vectorial polynomials of degree at most $p-1$ over T, and T is the triangle in $\widetilde{\mathcal{T}}_n(K)$ with $e \subset \partial T$ (this inequality holds true because the restriction of $\Pi_{p-1}^{0,T}(\nabla u)$ to e is a vectorial polynomial of degree $p-1$).

For any $v \in H^2(T)$, due to [35, Theorem 3.1], we have

$$\left\| \nabla v - \Pi_{p-1}^{0,T}(\nabla v) \right\|_{0,e} \leq \frac{\sqrt{5}+1}{\sqrt{2}} p^{-\frac{1}{2}} |\nabla v|_{1,T}. \tag{42}$$

Using that $\Pi^{0,T}_{p-1}\nabla q_p = \nabla q_p$ for all $q_p \in \mathbb{P}_p(T)$, owing to (42), we get

$$\left\| \nabla u - \Pi^{0,T}_{p-1}(\nabla u) \right\|_{0,e} = \left\| \left(\nabla\left(u - q_p\right)\right) - \Pi^{0,T}_{p-1}\left(\nabla\left(u - q_p\right)\right) \right\|_{0,e} \lesssim p^{-\frac{1}{2}} \left|\nabla\left(u - q_p\right)\right|_{1,T}.$$

Applying now standard hp-polynomial approximation results, see e.g. [17, Lemma 5.1], we obtain for every $q_p \in \mathbb{P}_p(T)$,

$$\left|\nabla\left(u - q_{p-1}\right)\right|_{1,T} \lesssim d^s\, p^{-s+1} |\nabla u|_{s,Q(T)}, \tag{43}$$

where d is a positive constant and $Q(T)$ is the parallelogram given by the union of T and its reflection defined above.

Moving to the second term in (41), assuming that $e = \partial T^- \cap \partial T^+$, where $T^\pm \in \widetilde{\mathcal{T}}_n$ and $T^\pm \subset K^\pm$, we have

$$\left\| [\![v_n]\!] - \Pi^{0,e}_{p-1} [\![v_n]\!] \right\|_{0,e} \le \left\| v_{n|_{T^+}} - \Pi^{0,T^+}_{p-1} v_{n|_{T^+}} \right\|_{0,e} + \left\| v_{n|_{T^-}} - \Pi^{0,T^-}_{p-1} v_{n|_{T^-}} \right\|_{0,e}.$$

Then, applying once again [35, Theorem 3.1], we deduce

$$\left\| [\![v_n]\!] - \Pi^{0,e}_{p-1} [\![v_n]\!] \right\|_{0,e} \lesssim p^{-\frac{1}{2}} \left(|v_{n|_{T^+}}|_{1,T^+} + |v_{n|_{T^-}}|_{1,T^-} \right).$$

By combining the bounds of the two terms on the right-hand side of (41) and the definition of the extended domain Ω_{ext} in (40), we get the assertion. □

We are now ready to state the main h- and p-error estimate result.

Theorem 3.6 *Let $\{\mathcal{T}_n\}_{n\in\mathbb{N}}$ be a sequence of polygonal decompositions satisfying **(D1)**–**(D4)**. Let u and u_n be the solutions to (2) and (10), respectively; we assume that u is the restriction to Ω of an H^{s+1}, $s \ge 1$, function (which we still denote u, with a slight abuse of notation), over Ω_{ext}, where Ω_{ext} is defined in (40). Then, the following a priori h- and p-error estimate holds true:*

$$|u - u_n|_{1,\mathcal{T}_n} \le c\, d^s \frac{\alpha^*(p)}{\alpha_*(p)}\, h^{\min(s,p)} \left\{ \left(\frac{\log(p)}{p} \right)^{\min_{K\in\mathcal{T}_n}(\lambda_K)\, s} + p^{-s} \right\} \|u\|_{s+1,\Omega_{\text{ext}}},$$

where c is a positive constant depending only on ρ_1, ρ_2, ρ_3, and Λ, d is a positive constant, $\lambda_K \pi$ denotes the smallest exterior angle of K for each $K \in \mathcal{T}_n$, and $\frac{\alpha^*(p)}{\alpha_*(p)}$ is the pollution factor appearing in (38), which is related to the choice of the stabilization.

Proof It is enough to combine Theorem 3.3 with Lemmata 3.4 and 3.5. □

Assuming, moreover, that u, the solution to the problem (2), is the restriction to Ω of an analytic function defined over Ω_{ext}, where Ω_{ext} was introduced in (40), it is possible to prove the following result.

Theorem 3.7 *Let **(D1)**–**(D4)** be valid and assume that u, the solution to the problem (2), is the restriction to Ω of an analytic function defined over Ω_{ext}, given in (40). Then, the following a priori p-error estimate holds true:*

$$|u - u_n|_{1,\mathcal{T}_n} \le c \exp\left(-b\, p\right),$$

for some positive constants b and c, depending again only on ρ_1, ρ_2, ρ_3, ρ_4 and Λ.

Proof It is enough to use Theorem 3.6, in combination with the tools employed in [17, Theorem 5.2]. □

Remark 6 The construction involving the collection of parallelograms in (40) is instrumental for proving Theorem 3.7. In order to derive the bound of Theorem 3.7 from that of Theorem 3.6, one needs to know the explicit dependence on s of the constant in the bound of Theorem 3.6. This comes at the price of involving the extended domain Ω_{ext}. If one were interested in approximating solutions with finite Sobolev regularity, then there would be no need of employing the construction with the parellelograms $Q(T)$. In particular, equation (43) would be valid also with the norm over the triangle T, instead of over $Q(T)$, on the right-hand side. As a consequence, the bounds in Lemma 3.5 and in Theorem 3.6 would be valid also with the norm of u over Ω, instead of over Ω_{ext}, on the right-hand sides. See [17] for additional details on the hp-version in the case of the standard VEM setting.

3.6 Error Estimates in the L^2 Norm

This section is devoted to bound the L^2 error of method (10) in terms of the energy error and best approximation error with respect to piecewise discontinuous harmonic polynomials. For simplicity, we restrict ourselves to the case of convex domains and of sequences of convex polygons; the non-convex case is discussed in Remark 7.

To this purpose, we firstly recall the definition of non-conforming VE spaces introduced in [7] for the approximation of the Poisson problem, and then we prove hp-best approximation estimates by functions in those spaces. The obtained results will be instrumental for proving L^2 error estimates for method (10). Throughout the whole section, we assume that p, the parameter used in the definition of local spaces (11), is equal to k, the non-conformity parameter, appearing in the definition of the global non-conforming VE space (7).

Let $K \in \mathcal{T}_n$. We define, for $p \in \mathbb{N}$ arbitrary,

$$V(K) := \left\{ v_n \in H^1(K) \mid \Delta v_n \in \mathbb{P}_{p-2}(K),\ (\nabla v_n \cdot \mathbf{n}_K)_{|_e} \in \mathbb{P}_{p-1}(e)\ \forall e \in \mathcal{E}_n \right\}.$$

It is proved in [7, Lemma 3.1] that the following is a set of degrees of freedom for the space $V(K)$. Given $v_n \in V(K)$, we associate the edge moments defined in (12)

$$\frac{1}{h_e} \int_e v_n m_\alpha^e \,\mathrm{d}s, \quad \forall \alpha = 0, \ldots, p-1,\ \forall e \in \mathcal{E}^K, \tag{44}$$

plus the bulk moments of the form

$$\frac{1}{|K|} \int_K v_n m_{\boldsymbol{\alpha}} \,\mathrm{d}x, \quad \forall |\boldsymbol{\alpha}| = 0, \ldots, p-2, \tag{45}$$

where $\{m_{\boldsymbol{\alpha}}\}_{|\boldsymbol{\alpha}|=0}^{p-2}$ is *any* basis of $\mathbb{P}_{p-2}(K)$.

For all $g \in H^{1/2}(\partial\Omega)$, the global non-conforming spaces in (7) are defined as in the harmonic case:

$$V_{n,g}^k := \left\{ v_n \in H_g^{1,nc}(\mathcal{T}_n, k) \mid v_{n|_K} \in V(K)\ \forall K \in \mathcal{T}_n \right\}. \tag{46}$$

The set of global degrees of freedom is obtained by a standard non-conforming coupling of the local counterparts. The precise treatment of Dirichlet boundary conditions should be dealt with as in Remark 2.

We want to show that, in the H^1 seminorm, the error between a regular target function and its interpolant in the space $V_{n,g}^p$ defined in (46) can be bounded by the best approximation error in the space of piecewise discontinuous polynomials of degree at most p. Notice that neither the convexity of Ω nor the convexity of the elements are needed here.

Proposition 3.8 *Given $g \in H^{1/2}(\partial\Omega)$, let $\psi \in V_g$, where V_g is defined in (3). For every polygonal partition $\mathcal{T}_n$ of Ω, there exists $\psi_I \in V^p_{n,g}$, with $V^p_{n,g}$ given in (46), such that*

$$|\psi - \psi_I|_{1,\mathcal{T}_n} \leq 2\left|\psi - q_p\right|_{1,\mathcal{T}_n} \quad \forall q_p \in \mathcal{S}^{p,-1}(\mathcal{T}_n),$$

where $\mathcal{S}^{p,-1}(\mathcal{T}_n)$ is the space of piecewise discontinuous polynomials, that is,

$$\mathcal{S}^{p,-1}(\mathcal{T}_n) := \left\{q \in L^2(\Omega) : q_{|K} \in \mathbb{P}_p(K)\, \forall K \in \mathcal{T}_n\right\}. \tag{47}$$

Proof The proof follows the lines of that of Proposition 3.1. Given $\psi \in V_g$, we define $\psi_I \in V^p_{n,g}$ by imposing its degrees of freedom as follows:

$$\begin{aligned} &\frac{1}{h_e}\int_e (\psi_I - \psi) q^e_{p-1}\,\mathrm{d}s = 0 \quad \forall q^e_{p-1} \in \mathbb{P}_{p-1}(e),\ \forall e \in \mathcal{E}^K,\ \forall K \in \mathcal{T}_n. \\ &\frac{1}{|K|}\int_K (\psi_I - \psi) q_{p-2}\,\mathrm{d}x = 0 \quad \forall q_{p-2} \in \mathbb{P}_{p-2}(K),\ \forall K \in \mathcal{T}_n, \end{aligned} \tag{48}$$

It is important to note that, since the degrees of freedom (44) and (45) are unisolvent for the space $V^p_{n,g}$, the interpolant ψ_I is defined in a unique way. Having this, we observe that, for all $K \in \mathcal{T}_n$,

$$|\psi - \psi_I|_{1,K} \leq |\psi - q_p|_{1,K} + |\psi_I - q_p|_{1,K} \quad \forall q_p \in \mathbb{P}_p(K).$$

We focus on the second term. By integration by parts we get

$$\begin{aligned} |\psi_I - q_p|^2_{1,K} &= \int_K -\Delta(\psi_I - q_p)(\psi_I - q_p)\,\mathrm{d}x + \int_{\partial K} \nabla(\psi_I - q_p)\cdot \mathbf{n}_K\,(\psi_I - q_p)\,\mathrm{d}s \\ &= \int_K -\Delta(\psi_I - q_p)(\psi - q_p)\,\mathrm{d}x + \int_{\partial K} \nabla(\psi_I - q_p)\cdot \mathbf{n}_K\,(\psi - q_p)\,\mathrm{d}s, \end{aligned}$$

where, in the last identity, the definition of the non-conforming space $V^p_{n,g}$, given in (46) and the definition (48) of ψ_I via the degrees of freedom were used. Integrating by parts back, we obtain

$$|\psi_I - q_p|^2_{1,K} = \int_K \nabla(\psi_I - q_p)\cdot\nabla(\psi - q_p)\,\mathrm{d}x \leq |\psi_I - q_p|_{1,K}|\psi - q_p|_{1,K}.$$

This concludes the proof. □

We are now ready to prove a bound of the L^2 error of the method. We will assume henceforth that Ω is a convex domain split into a collection of convex polygons. An analogous analysis could be performed in the non-convex case, and slightly worse error estimates could be proven, see Remark 7. Nonetheless, here we stick to the convex setting, since we deem it is clearer.

Theorem 3.9 *Let Ω be a polygonal convex domain and let $\{\mathcal{T}_n\}_{n\in\mathbb{N}}$ be a sequence of decompositions into convex polygons satisfying (**D1**)–(**D4**). Let u and u_n be the solutions to (2) and (10), respectively; we assume that u is the restriction to Ω of a H^{s+1}, $s \geq 1$, function (which we still denote, with a slight abuse of notation, u) over Ω_{ext}, where Ω_{ext} is defined in (40). Then,*

$$\begin{aligned} \|u - u_n\|_{0,\Omega} \leq c \Bigg\{ &\frac{h^{\min(s,p)+1}}{p^{s+1}}\|u\|_{s+1,\Omega_{\text{ext}}} \\ &+ \max\left(\frac{h}{p}, h\,\alpha^*(p)\left(\frac{\log(p)}{p}\right)^{\max_{K\in\mathcal{T}_n}\lambda_K}\right)\left(|u - u_n|_{1,\mathcal{T}_n} + \inf_{q_p^\Delta \in \mathcal{S}^{p,\Delta,-1}(\mathcal{T}_n)}\left|u - q_p^\Delta\right|_{1,\mathcal{T}_n}\right)\Bigg\}, \end{aligned}$$

where c is a positive constant depending only on ρ_1, ρ_2, ρ_3, ρ_4 and Λ, $\alpha^*(p)$ is the "upper" stability constant appearing in (25), $\mathcal{S}^{p,\Delta,-1}(\mathcal{T}_n)$ is defined in (17), and $\lambda_K\pi$ denotes the smallest exterior angle of K for each $K \in \mathcal{T}_n$.

Proof We consider the following dual problem: Find $\psi \in H^1(\Omega)$ such that

$$\begin{cases} -\Delta\psi = u - u_n & \text{in } \Omega \\ \psi = 0 & \text{on } \partial\Omega. \end{cases} \tag{49}$$

Standard stability and a priori regularity theory implies that $\psi \in H^2(\Omega)$ and

$$\|\psi\|_{2,\Omega} \lesssim \|u - u_n\|_{0,\Omega}, \tag{50}$$

where the hidden constant depends only on the domain Ω, see e.g. [44, Theorem 3.2.1.2].

Using (49) and (37), and taking into account that $u - u_n \in H_0^{1,nc}(\mathcal{T}_n, p)$, we obtain the following equivalent expression for the L^2 error:

$$\begin{aligned} \|u - u_n\|_{0,\Omega}^2 &= \sum_{K\in\mathcal{T}_n} \int_K (-\Delta\psi)(u - u_n)\,\mathrm{d}x \\ &= \sum_{K\in\mathcal{T}_n} \left\{ \int_K \nabla\psi \cdot \nabla(u - u_n)\,\mathrm{d}x - \int_{\partial K} \nabla\psi \cdot \mathbf{n}_K\,(u - u_n)\,\mathrm{d}s \right\} \\ &= \sum_{K\in\mathcal{T}_n} a^K(\psi - \psi_I, u - u_n) + \sum_{K\in\mathcal{T}_n} a^K(\psi_I, u - u_n) - \mathcal{N}_n(\psi, u - u_n) \\ &=: T_1 + T_2 + T_3, \end{aligned} \tag{51}$$

where ψ_I is the (unique) function in $V_{n,0}^p$, the enlarged space of functions with zero Dirichlet traces introduced in (46), defined from ψ via (48); in particular, ψ_I is not piecewise harmonic, in general.

We begin by bounding term T_1. Owing to the Cauchy–Schwarz inequality and Proposition 3.8, we have

$$|T_1| \le |\psi - \psi_I|_{1,\mathcal{T}_n}|u - u_n|_{1,\mathcal{T}_n} \le 2|\psi - q_p|_{1,\mathcal{T}_n}|u - u_n|_{1,\mathcal{T}_n} \quad \forall q_p \in \mathcal{S}^{p,-1}(\mathcal{T}_n),$$

where $\mathcal{S}^{p,-1}(\mathcal{T}_n)$ is the space of piecewise discontinuous polynomials introduced in (47). By taking q_p equal to the best approximation of ψ in $\mathcal{S}^{p,-1}(\mathcal{T}_n)$ and using [17, Lemma 4.2], together with (50), we have

$$|T_1| \lesssim \frac{h}{p}\|\psi\|_{2,\Omega}|u - u_n|_{1,\mathcal{T}_n} \lesssim \frac{h}{p}\|u - u_n\|_{0,\Omega}|u - u_n|_{1,\mathcal{T}_n}.$$

Next, we focus on term T_3 on the right-hand side of (51). Following the same steps as in the proof of Lemma 3.5, we obtain

$$|T_3| = |\mathcal{N}_n(\psi, u - u_n)| \le \sum_{e\in\mathcal{E}_n} \left\| \nabla\psi - \Pi_{p-1}^{0,e}(\nabla\psi) \right\|_{0,e} \left\| [\![u - u_n]\!] - \Pi_{p-1}^{0,e}[\![u - u_n]\!] \right\|_{0,e},$$

where $\Pi_{p-1}^{0,e}$ denotes here again, with an abuse of notation, the L^2 projector onto vectorial polynomial spaces. Applying [35, Theorem 3.1] and [17, Lemma 4.1] similarly as in the proof of Lemma 3.5, together with (50) ($|\nabla\psi|_{1,K} \le \|\psi\|_{2,K}$), we get

$$|T_3| \lesssim \frac{h}{p}\|u - u_n\|_{0,\Omega}|u - u_n|_{1,\mathcal{T}_n}.$$

Finally, we study term T_2 on the right-hand side of (51), which can be split as

$$T_2 = \sum_{K\in\mathcal{T}_n} a^K(\psi_I, u - u_n) = \sum_{K\in\mathcal{T}_n} a^K(u, \psi_I) - \sum_{K\in\mathcal{T}_n} a^K(u_n, \psi_I) =: T_4 + T_5. \qquad (52)$$

The first term T_4 is related to the non-conformity of the discretization spaces, whereas the second term T_5 reflects the fact that method (10) does not employ the original bilinear form.

We start to bound term T_4. Using computations analogous to those in the proof of Lemma 3.5, it is possible to deduce

$$\begin{aligned}|T_4| &= \left|\sum_{K\in\mathcal{T}_n} a^K(u, \psi_I)\right| = \left|\sum_{K\in\mathcal{T}_n} \int_{\partial K} \nabla u \cdot \mathbf{n}_K\, \psi_I \,\mathrm{d}s\right| = |\mathcal{N}_n(u, \psi_I)| = |\mathcal{N}_n(u, \psi_I - \psi)|\\ &\leq \sum_{e\in\mathcal{E}_n} \left\|\nabla u - \Pi^{0,e}_{p-1}(\nabla u)\right\|_{0,e} \left\|[\![\psi_I - \psi]\!] - \Pi^{0,e}_{p-1}[\![\psi_I - \psi]\!]\right\|_{0,e},\end{aligned}$$

where in the fourth identity we used the fact that $\mathcal{N}_n(u, \psi) = 0$, which holds since u and ψ are sufficiently regular, and in the last step we used (41). Again, $\Pi^{0,e}_{p-1}$ has to be understood as the L^2 projection onto the vectorial polynomial spaces of degree at most $p-1$ on e. Applying [35, Theorem 3.1], Proposition 3.8, [17, Lemma 4.2], and finally (50), leads to

$$|T_4| \lesssim p^{-1} |\nabla\left(u - \Pi^{\nabla}_p u\right)|_{1,\mathcal{T}_n} |\psi - \psi_I|_{1,\mathcal{T}_n} \lesssim \frac{h^{\min(s,p)}}{p^s} \|u\|_{s+1,\Omega_{\mathrm{ext}}} \frac{h}{p} \|u - u_n\|_{0,\Omega},$$

where we recall that Ω_{ext} is defined in (40) and where Π^{∇}_p is any piecewise energy projector from $H^1(K)$ into $\mathbb{P}_p(K)$, for all $K \in \mathcal{T}_n$.

Finally, it remains to treat term T_5 on the right-hand side of (52). To this purpose, we consider the following splittings of ψ and ψ_I. Firstly, we split ψ into $\psi = \psi^1 + \psi^2$, where ψ^1 and ψ^2 are, element by element, solutions to the local problems

$$\begin{cases} -\Delta\psi^1 = -\Delta\psi & \text{in } K\\ \psi^1 = 0 & \text{on } \partial K, \end{cases} \qquad \begin{cases} -\Delta\psi^2 = 0 & \text{in } K\\ \psi^2 = \psi & \text{on } \partial K \end{cases} \qquad (53)$$

for all $K \in \mathcal{T}_n$. Using (49), we can also observe that $\psi^2 - \psi$ solve the local problems

$$\begin{cases} -\Delta(\psi - \psi^2) = u - u_n & \text{in } K\\ \psi - \psi^2 = 0 & \text{on } \partial K, \end{cases}$$

Then, (local) standard a priori regularity theory and, afterwards, summation over all elements $K \in \mathcal{T}_n$ imply the global bound

$$\|\psi^2 - \psi\|_{2,\mathcal{T}_n} \lesssim \|u - u_n\|_{0,\Omega}, \qquad (54)$$

where the broken norm $\|\cdot\|_{2,\mathcal{T}_n}$ is defined in (5). With the triangle inequality, (50), and (54), we get

$$\|\psi^2\|_{2,\mathcal{T}_n} \leq \|\psi - \psi^2\|_{2,\mathcal{T}_n} + \|\psi\|_{2,\Omega} \lesssim \|u - u_n\|_{0,\Omega}. \qquad (55)$$

Secondly, we split $\psi_I \in V^p_{n,0}$ into $\psi_I = \psi_I^1 + \psi_I^2$. We define ψ_I^2 as the unique element in $V^{\Delta,p}_{n,0}$ introduced in (16), which satisfies

$$\frac{1}{h_e}\int_e \psi_I^2 q^e_{p-1}\,\mathrm{d}s = \frac{1}{h_e}\int_e \psi_I q^e_{p-1}\,\mathrm{d}s \quad \forall q^e_{p-1} \in \mathbb{P}_{p-1}(e),\ \forall e \in \mathcal{E}_n. \qquad (56)$$

Existence and uniqueness of ψ_I^2 follow from the fact that we are defining ψ_I^2 via unisolvent degrees of freedom for the space $V_{n,0}^{\Delta,p}$. Owing to (56), the definition of ψ_I in (48), and (53), we deduce

$$\frac{1}{h_e}\int_e \psi_I^2 q_{p-1}^e \, \mathrm{d}s = \frac{1}{h_e}\int_e \psi_I q_{p-1}^e \, \mathrm{d}s = \frac{1}{h_e}\int_e \psi q_{p-1}^e \, \mathrm{d}s$$
$$= \frac{1}{h_e}\int_e \psi^2 q_{p-1}^e \, \mathrm{d}s \quad \forall q_{p-1}^e \in \mathbb{P}_{p-1}(e),\ \forall e \in \mathcal{E}_n.$$

This entails that ψ_I^2 approximates ψ^2 in the sense of Proposition 3.1. Having this, the function $\psi_I^1 = \psi_I - \psi_I^2 \in V_{n,0}^{p}$ satisfies

$$\begin{cases} \dfrac{1}{|e|}\displaystyle\int_e \psi_I^1 q_{p-1}^e \, \mathrm{d}s = 0 & \forall q_{p-1}^e \in \mathbb{P}_{p-1}(e),\ \forall e \in \mathcal{E}^K,\ \forall K \in \mathcal{T}_n, \\ \dfrac{1}{|K|}\displaystyle\int_K \psi_I^1 q_{p-2} \, \mathrm{d}x = \dfrac{1}{|K|}\displaystyle\int_K \left(\psi_I - \psi_I^2\right) q_{p-2} \, \mathrm{d}x & \forall q_{p-2} \in \mathbb{P}_{p-2}(K),\ \forall K \in \mathcal{T}_n. \end{cases}$$

Moreover, since $u_n \in V_{n,g}^{\Delta,k}$, ψ_I^1 has the essential feature that it satisfies

$$a^K\left(u_n, \psi_I^1\right) = \int_K \Bigg(\underbrace{-\Delta u_n}_{=0}\Bigg) \psi_I^1 \, \mathrm{d}x + \underbrace{\int_{\partial K} \left(\nabla u_n \cdot \mathbf{n}_K\right) \psi_I^1 \, \mathrm{d}s}_{=0} = 0. \tag{57}$$

We have now all the tools for bounding term T_5. Using (57), (10), and (24), we get

$$\begin{aligned} |T_5| &= \left| \sum_{K \in \mathcal{T}_n} a^K\left(u_n, \psi_I^2\right) \right| = \left| \sum_{K \in \mathcal{T}_n} \left\{ a_n^K\left(u_n, \psi_I^2\right) - a^K\left(u_n, \psi_I^2\right) \right\} \right| \\ &= \left| \sum_{K \in \mathcal{T}_n} \left\{ a_n^K\left(u_n - q_p^\Delta, \psi_I^2 - \widetilde{q}_p^\Delta\right) - a^K\left(u_n - q_p^\Delta, \psi_I^2 - \widetilde{q}_p^\Delta\right) \right\} \right| \\ &\quad \forall q_p^\Delta,\ \widetilde{q}_p^\Delta \in \mathcal{S}^{p,\Delta,-1}(\mathcal{T}_n), \end{aligned}$$

where we recall that $\mathcal{S}^{p,\Delta,-1}(\mathcal{T}_n)$ is defined in (17). It is important to highlight that it is in fact a key point of the error analysis to have piecewise harmonic functions in both entries of the discrete bilinear form. By applying the continuity property (26) and the Cauchy–Schwarz inequality, then the triangle inequality and Proposition 3.1, we deduce

$$\begin{aligned} |T_5| &\lesssim \alpha^*(p) \left| u_n - q_p^\Delta \right|_{1,\mathcal{T}_n} \left| \psi_I^2 - \widetilde{q}_p^\Delta \right|_{1,\mathcal{T}_n} \\ &\le \alpha^*(p) \left(|u - u_n|_{1,\mathcal{T}_n} + \left| u - q_p^\Delta \right|_{1,\mathcal{T}_n} \right) \left(\left|\psi^2 - \psi_I^2\right|_{1,\mathcal{T}_n} + \left| \psi^2 - \widetilde{q}_p^\Delta \right|_{1,\mathcal{T}_n} \right) \\ &\lesssim \alpha^*(p) \left(|u - u_n|_{1,\mathcal{T}_n} + \left| u - q_p^\Delta \right|_{1,\mathcal{T}_n} \right) \left| \psi^2 - \widetilde{q}_p^\Delta \right|_{1,\mathcal{T}_n}. \end{aligned}$$

Thanks to Lemma 3.4 (here, $s = 1$) and the bound (55), we have

$$|T_5| \lesssim \alpha^*(p) \left(|u - u_n|_{1,\mathcal{T}_n} + \left| u - q_p^\Delta \right|_{1,\mathcal{T}_n} \right) h \left(\frac{\log(p)}{p} \right)^{\min_{K \in \mathcal{T}_n} \lambda_K} \left(\sum_{K \in \mathcal{T}_n} \| \psi^2 \|_{2,K}^2 \right)^{\frac{1}{2}}$$

$$\lesssim \alpha^*(p) \left(|u - u_n|_{1,\mathcal{T}_n} + \left| u - q_p^\Delta \right|_{1,\mathcal{T}_n} \right) h \left(\frac{\log(p)}{p} \right)^{\min_{K \in \mathcal{T}_n} \lambda_K} \| u - u_n \|_{0,\Omega} ,$$

where we recall that, for any $K \in \mathcal{T}_n$, $\lambda_K \pi$ denotes the smallest exterior angle of K.

By combining the estimates on all the terms T_1 to T_5, we get the assertion. □

Remark 7 As already highlighted, the case of non-convex Ω can be treated analogously. More precisely, given ω the largest reentrant angle of Ω, the solution of (2) belongs to $H^{1+t}(\Omega)$, with $t = \frac{\pi}{\omega} - \varepsilon$ for all $\varepsilon > 0$ arbitrarily small. Standard stability and a priori regularity theory, see [9, Theorem 2.1], gives

$$\| \psi \|_{1+t,\Omega} \leq c \| u - u_n \|_{0,\Omega}$$

for some positive constant c depending only on the domain Ω. An analogous bound is valid for the counterpart of (54) in the non-convex case. Having this, a straightforward modification of the proof of Theorem 3.9 leads to the h- and p-error bounds

$$\| u - u_n \|_{0,\Omega} \leq \Bigg\{ c \, \frac{h^{\min(s,p)+t}}{p^{s+t}} \| u \|_{s+1,\Omega_{\text{ext}}} + \max \left(\left(\frac{h}{p} \right)^t , \, h^t \alpha^*(p) \left(\frac{\log(p)}{p} \right)^{\max_{K \in \mathcal{T}_n} (\lambda_K) \, t} \right) \cdot \left(|u - u_n|_{1,\mathcal{T}_n} + \inf_{q_p^\Delta \in \mathcal{S}^{p,\Delta,-1}(\mathcal{T}_n)} |u - q_p^\Delta|_{1,\mathcal{T}_n} \right) \Bigg\} ,$$

where c is a positive constant depending only on the constants ρ_1, ρ_2, ρ_3, ρ_4, and Λ appearing in (**D1**)–(**D4**) and in the proof of Lemma 3.5.

The presence of non-convex polygons in the decomposition $\mathcal{T}_n$ leads to a possible additional loss in the convergence rate in p of the L^2 error, which will depend on the largest interior and exterior angles of the polygons.

3.7 Hints for the Extension to the 3D Case

The aim of this section is to give a hint concerning the extension of what we have presented and discussed so far to the three dimensional case.

Concerning the definition of local harmonic VE spaces, one mimics the strategy suggested in [7] and defines, for every polyhedron K in $\mathbb{R}^3$ and any fixed $p \in \mathbb{N}$,

$$V^\Delta(K) := \left\{ v_n \in H^1(K) \mid \Delta v_n = 0 \text{ in } K, \; (\nabla v_n \cdot \mathbf{n}_K)_{|F} \in \mathbb{P}_{p-1}(F) \; \forall F \text{ faces of } K \right\}.$$

We observe that the definition of the local 3D space is a straightforward extension of its 2D counterpart. We underline that this is not the case when using *conforming* VEM. In that case, typically, one also requires to have a modified version of the local VE spaces on each face, see [2]. On the one hand, this allows the construction of continuous functions over the boundary of a polyhedron, as well as the construction of projectors onto proper polynomial spaces; on the other, it complicates the p-analysis of the method. In the non-conforming framework, however, one does not need to fix any sort of continuity across the interface between faces of a polyhedron and thus it suffices to impose that normal derivatives are polynomials.

The global 3D non-conforming space is built as in the 2D case. Also, the degrees of freedom are given by scaled face moments with respect to polynomials up to order $p-1$.

The abstract definition of the 2D local discrete bilinear form in (23) can also be employed in the 3D case. The (properly scaled) 3D counterpart of the 2D explicit stabilization defined in (28) would be

$$S^K(u_n, v_n) = \sum_{F \text{ faces of } K} \frac{p}{h_F} \left(\Pi^{0,F}_{p-1} u_n, \Pi^{0,F}_{p-1} v_n \right)_{0,F},$$

where, for any face F, $\Pi^{0,F}_{p-1}$ denotes the L^2 projector onto $\mathbb{P}_{p-1}(F)$ of the traces on F of functions in the 3D VE space. Nonetheless, it is not clear whether explicit bounds in terms of p of the stability constants appearing in (22) can be proved for this form. In fact, in the 2D case, hp-polynomial inverse estimates in 1D were the key tool for proving Theorem 3.2. In the 3D framework, one needs to employ hp-polynomial inverse estimates on general polygons based on weighted norms. We highlight that the approach of [31, Chapter 3], see also [30], could be followed in order to prove such hp-weighted inverse inequalities. However, as this extension is quite technical, we do not investigate it here.

Independently of the specific choice of the stabilization, provided that it is symmetric and satisfies (25), the abstract error analysis is dealt with similarly to the 2D case, see Theorem 3.3. The only modification is in the definition of the non-conformity term, which in 3D is defined as

$$\mathcal{N}_n(u, v) = \sum_{F \in \mathcal{E}_n^3} \int_F \nabla u \cdot [\![v]\!]_F \, \mathrm{d}s$$

for all conforming functions u and all non-conforming functions v, where $\mathcal{E}_n^3$ denotes the set of faces in the polyhedral decomposition, and $[\![\cdot]\!]_F$ is defined as in (6) in terms of normal derivatives over faces.

The proof of h- and p-error bounds for this non-conforming term follows the same lines as in the 2D case, since [35, Theorem 3.1] holds true on simplices in arbitrary space dimension. For the best approximation error, one should use the 3D version of Lemma 3.4, which can be found e.g. in [52, Theorem 3.12].

4 Numerical Results

We present in Sect. 4.1 some numerical tests for the h-version and the p-version of the method, validating the theoretical results obtained in Sect. 3; we conclude with a discussion and some tests on the hp-version in Sect. 4.2. As already mentioned, we refer to “Appendix A” for details on the implementation of the method.

4.1 Numerical Results: *h*- and *p*-Version

In this section, we present numerical experiments validating the theoretical error estimates in the $H^1(\mathcal{T}_n)$ (H^1, for short) and L^2 norms discussed in Theorems 3.6, 3.7, and 3.9.

For the following numerical experiments, we consider boundary value problems of the form (1), on $\Omega := (0, 1)^2$, with known exact solutions given by

- $u_1(x, y) = e^x \sin(y)$,
- $u_2(x, y) = u_2(r, \theta) = r^2 (\log(r) \sin(2\theta) + \theta \cos(2\theta))$.

We underline that u_1 is an analytic function in Ω, whereas $u_2 \in H^{3-\epsilon}(\Omega)$ for every $\epsilon > 0$ arbitrarily small; moreover, u_2 represents the natural singular solution at $\mathbf{0} = (0, 0)$ of the Poisson problem on a square domain, see e.g. [9].

We discretize these problems on sequences of quasi-uniform Cartesian meshes and Voronoi-Lloyd meshes of the type shown in Fig. 2, left and center, respectively. We also test on a problem with exact solution u_1 on the domain Ω given by the union of four Escher horses as in Fig. 2, right.

It is important to note that, since an explicit representation of the numerical approximation u_n inside each element is not available, due to the "virtuality" of the basis functions, we cannot compute the L^2 and H^1 errors of the method directly. Instead, we will compute the following relative errors between u and $\Pi^\nabla_p u_n$, Π^∇_p being defined in (15):

$$\frac{\left\| u - \Pi^\nabla_p u_n \right\|_{0,\Omega}}{\|u\|_{0,\Omega}}, \quad \frac{\left\| u - \Pi^\nabla_p u_n \right\|_{1,\mathcal{T}_n}}{\|u\|_{1,\Omega}}. \tag{58}$$

We observe that the "computable" H^1 error in (58) is related to the exact H^1 error. In fact, thanks to Theorem 3.3, we have

$$\begin{aligned} |u - u_n|_{1,\mathcal{T}_n} &\lesssim \inf_{q_p^\Delta \in \mathcal{S}^{p,\Delta,-1}(\mathcal{T}_n)} \left| u - q_p^\Delta \right|_{1,\mathcal{T}_n} + \sup_{v_n \in V_{n,0}^{\Delta,p}} \frac{\mathcal{N}_n(u, v_n)}{|v_n|_{1,\mathcal{T}_n}} \\ &\leq \left| u - \Pi^\nabla_p u_n \right|_{1,\mathcal{T}_n} + \sup_{v_n \in V_{n,0}^{\Delta,p}} \frac{\mathcal{N}_n(u, v_n)}{|v_n|_{1,\mathcal{T}_n}}; \end{aligned}$$

the convergence of the second term on the right-hand side is provided in Lemma 3.5. Moreover, by the triangle inequality and the stability of the H^1-projection, one also has

$$\begin{aligned} \left| u - \Pi^\nabla_p u_n \right|_{1,\mathcal{T}_n} &\leq \left| u - \Pi^\nabla_p u \right|_{1,\mathcal{T}_n} + \left| \Pi^\nabla_p (u - u_n) \right|_{1,\mathcal{T}_n} \\ &\leq \left| u - \Pi^\nabla_p u \right|_{1,\mathcal{T}_n} + |u - u_n|_{1,\mathcal{T}_n}; \end{aligned}$$

the convergence of the second term on the right-hand side is provided in Lemma 3.4.

4.1.1 Numerical Results: *h*-Version

In this section, we verify the algebraic rate of convergence of the h-version of the method, validating thus Theorems 3.6 and 3.9 for different degrees of accuracy $p = 1, 2, 3, 4, 5$ of the method.

The numerical results for the problems in $\Omega = (0, 1)^2$ with exact solutions u_1 and u_2, obtained on sequences of Cartesian and Voronoi-Lloyd meshes, are depicted in Figs. 3 and 4.

From Theorems 3.6 and 3.9, we expect the H^1 and L^2 errors to behave like $\mathcal{O}(h^{\min(t,p)})$ and $\mathcal{O}(h^{\min(t,p)+1})$, respectively, where $t + 1$ is the regularity of the exact solution u, and p is the degree of accuracy. The numerical results in Figs. 3 and 4 are in agreement with these

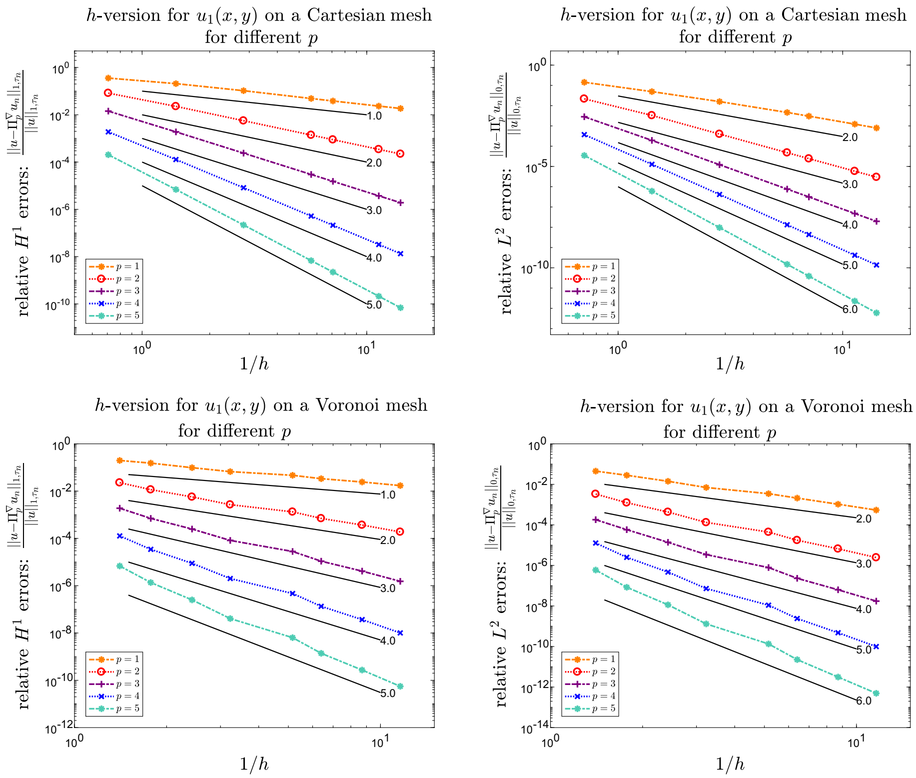

Fig. 3 Convergence of the h-version of the method for the analytic solution u_1 on quasi-uniform Cartesian (first row) and Voronoi-Lloyd (second row) meshes; relative H^1 errors (left) and relative L^2 errors (right) defined in (58)

theoretical estimates. In fact, for u_1, which belongs to $H^s(\Omega)$ for all $s \geqslant 0$, we see that the H^1 error actually converges with order $\mathcal{O}(h^p)$, and the L^2 error with order $\mathcal{O}(h^{p+1})$ for all degrees of accuracy. On the other hand, we observe convergence rates 1 and 2, respectively, for $p = 1$, and convergence rates 2 and 3, respectively, for $p = 2, 3, 4, 5$. This is due to the fact that the expected convergence is of order $\mathcal{O}(h^{\min\{2-\epsilon, p\}})$ in the H^1 norm and $\mathcal{O}(h^{\min\{2-\epsilon, p\}+1})$ in the L^2 norm.

4.1.2 Numerical Results: *p*-Version

In this section, we validate the exponential convergence of the p-version of the method for the model problem (1) with exact solution u_1 on $\Omega = (0, 1)^2$ on a Cartesian mesh and a Voronoi mesh made of four elements, respectively, as well as on the domain Ω given by the union of four Escher horses (see Fig. 2, right). The obtained results are depicted in Fig. 5, where the logarithm of the relative errors defined in (58) is plotted against the polynomial degree p.

One can clearly observe that the exponential convergence predicted in Theorem 3.7 is attained, even when employing a very coarse mesh with (non-convex) non-star-shaped elements, as the one in Fig. 2, right.

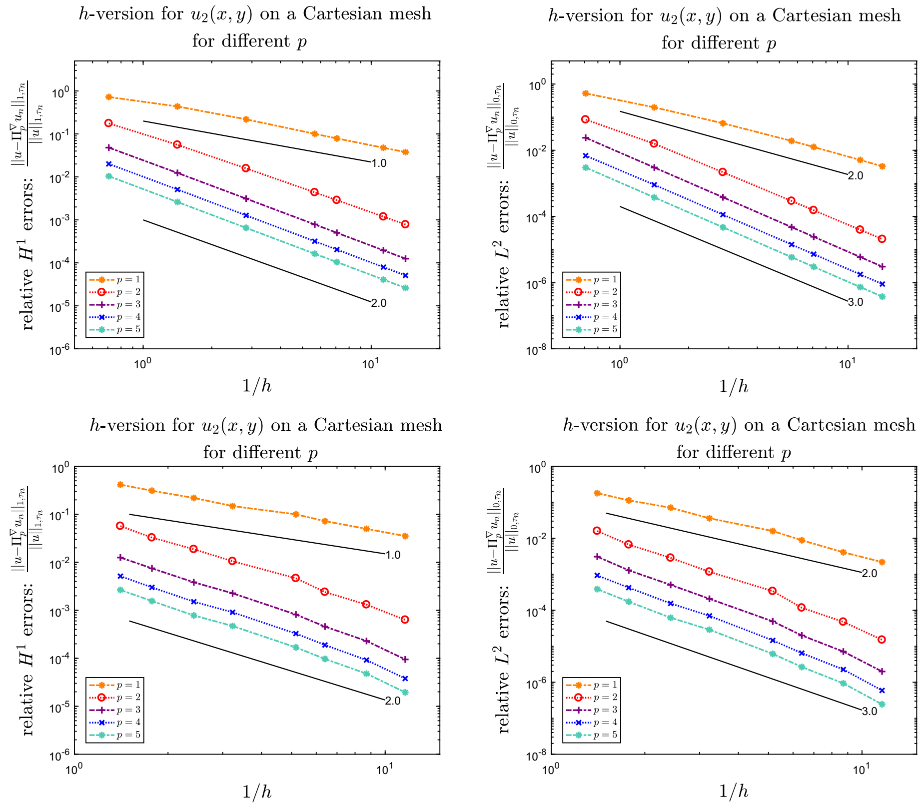

Fig. 4 Convergence of the h-version of the method for the solution u_2 with finite Sobolev regularity on quasi-uniform Cartesian (first row) and Voronoi-Lloyd (second row) meshes; relative H^1 errors (left) and relative L^2 errors (right) defined in (58)

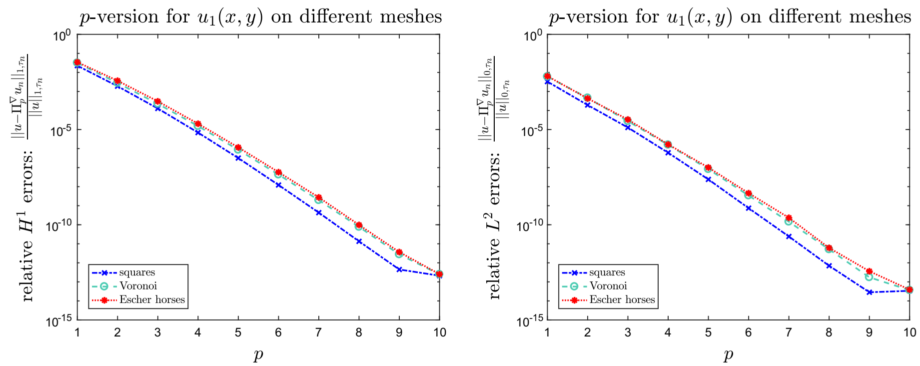

Fig. 5 Convergence of the p-version of the method for the analytic solution u_1 on a quasi-uniform Cartesian mesh, a Voronoi-Lloyd mesh, and a Escher horses mesh; relative H^1 errors (left) and relative L^2 errors (right) defined in (58)

4.2 The *hp*-Version and Approximation of Corner Singularities

So far, both the theoretical analysis and the numerical tests were performed considering approximation spaces with uniform degree of accuracy p and with quasi-uniform meshes.

In general, however, the solutions to elliptic problems over polygonal domains have natural singularities arising in neighbourhoods of the corners of the domain. In particular, for problem (2) in a domain Ω with reentrant corners, the solution might have a regularity lower than H^2, even if the Dirichlet boundary datum g is smooth; for a precise functional setting regarding regularity of solutions to elliptic PDEs, we refer to [9,44,56] and the references therein. This implies that both the h- and the p-versions of standard Galerkin methods, in general, have limited approximation properties. In particular, employing quasi-uniform meshes and uniform degree of accuracy, does not entail any sort of exponential convergence.

A possible way to recover exponential convergence, even in presence of corner singularities, is to use the so-called hp-strategy firstly designed by Babuška and Guo [8–10] in the FEM framework, and then generalized to the VEM in [18]. This strategy consists in combining mesh refinement towards the corners of the domain and increasing the number of degrees of freedom over the polygonal decomposition in a non-uniform way. In this section, we discuss and numerically test an hp-version of the presented non-conforming harmonic VEM.

To this purpose, we recall the concept of sequences of geometrically graded polygonal meshes $\{\mathcal{T}_n\}_{n\in\mathbb{N}}$. For a given $n \in \mathbb{N}$, $\mathcal{T}_n$ is a polygonal mesh consisting of $n+1$ layers, where we define a *layer* as follows. The so-called 0-th layer is the set of all polygons in $\mathcal{T}_n$ abutting the vertices of Ω. The other layers are defined inductively by requiring that the ℓ-th layer consists of those polygons, which abut the polygons in the $(\ell-1)$-th layer. More precisely, for all $\ell = 1, \ldots, n$, we set

$$L_{n,\ell} := L_\ell := \left\{ K \in \mathcal{T}_n \mid \overline{K} \cap \overline{K_{\ell-1}} \neq \emptyset \text{ for some } K_{\ell-1} \in L_{\ell-1},\ K \not\subseteq \cup_{j=0}^{\ell-1} L_j \right\}.$$

The hp-gospel states that, in order to achieve exponential convergence of the error, one has to employ geometrically graded sequences of meshes. For this reason, we consider sequences $\{\mathcal{T}_n\}_{n\in\mathbb{N}}$ satisfying (**D1**)–(**D3**), but not (**D4**); we require instead

(**D5**) for all $n \in \mathbb{N}$, there exists $\sigma \in (0,1)$, called *grading parameter*, such that

$$h_K \approx \begin{cases} \sigma^n & \text{if } K \in L_0 \\ \frac{1-\sigma}{\sigma} \operatorname{dist}\left(K, \mathcal{V}^\Omega\right) & \text{if } K \in L_\ell,\ \ell = 1, \ldots, n, \end{cases} \tag{59}$$

where $\mathcal{V}^\Omega$ denotes the set of vertices of the polygonal domain Ω.

Sequences $\{\mathcal{T}_n\}_{n\in\mathbb{N}}$ satisfying (**D5**) have the property that the layers “near” the corners of the domain consist of elements with measure converging to zero, whereas the other layers consist of polygons with fixed size. In Fig. 6, we depict three meshes that represent the third elements $\mathcal{T}_3$ in certain sequences of meshes of the L-shaped domain

$$\Omega := (-1,1)^2 \setminus (-1,0)^2, \tag{60}$$

which are graded, for simplicity, only towards the vertex $\mathbf{0}$.

We still miss a crucial ingredient for a complete description of the hp-strategy, namely harmonic VE spaces with non-uniform degrees of accuracy. For all $n \in \mathbb{N}$, we can order the elements in $\mathcal{T}_n$ as $K_1, K_2, \ldots, K_{\mathrm{card}(\mathcal{T}_n)}$; then we consider a vector $\mathbf{p}_n \in \mathbb{N}^{\mathrm{card}(\mathcal{T}_n)}$ whose entries are defined as follows:

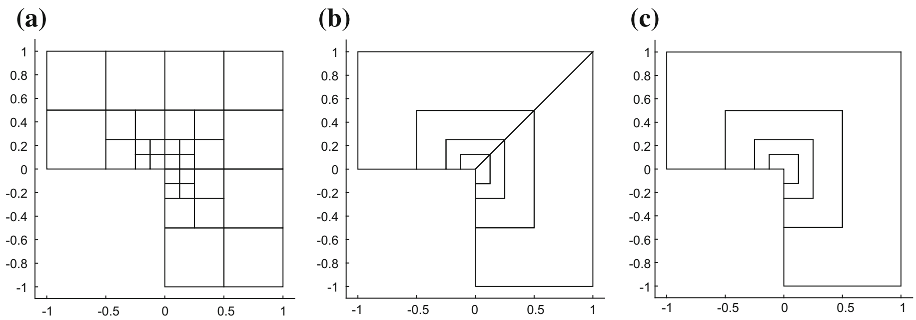

Fig. 6 Third element $\mathcal{T}_3$ in three different sequences of geometrically graded meshes (type **a**–**c** from left to right) with $\sigma = 0.5$

$$(\mathbf{p}_n)_j := \begin{cases} 1 & \text{if } K_j \in L_0 \\ \max(1, \lceil \mu(\ell+1) \rceil) & \text{if } K_j \in L_\ell,\ \ell = 1, \ldots, n, \end{cases} \tag{61}$$

where μ is a positive parameter to be assigned, and where $\lceil \cdot \rceil$ is the ceiling function.

Having $\mathbf{p}_n$ for all $n \in \mathbb{N}$, we consider the elements e_1, e_2, ..., $e_{\mathrm{card}(\mathcal{E}_n)}$ in $\mathcal{E}_n$; we consequently define a vector $\mathbf{p}_n^{\mathcal{E}} \in \mathbb{N}^{\mathrm{card}(\mathcal{E}_n)}$, whose entries are built using the following rule (*maximum rule*):

$$\left(\mathbf{p}_n^{\mathcal{E}}\right)_j := \begin{cases} (\mathbf{p}_n)_i & \text{if } e_j \in \mathcal{E}_n^B \text{ and } e_j \subset \partial K_i \\ \max\left((\mathbf{p}_n)_{i_1}, (\mathbf{p}_n)_{i_2}\right) & \text{if } e_j \in \mathcal{E}_n^I \text{ and } e_j \subset \partial K_{i_1} \cap \partial K_{i_2}. \end{cases}$$

At this point, we define the local harmonic VE spaces with non-uniform degrees of accuracy as follows. For all $K \in \mathcal{T}_n$, we set

$$V^\Delta(K) := \left\{ v_n \in H^1(K) \mid \Delta v_n = 0 \text{ in } K,\ (\nabla v_n \cdot \mathbf{n}_K)_{|e_j} \in \mathbb{P}_{\left(\mathbf{p}_n^{\mathcal{E}}\right)_j}(e_j)\, \forall e_j \text{ edge of } K \right\}.$$

The global non-conforming space and the set of global degrees of freedom are defined similarly to those for the case of uniform degree, see Sect. 3. The difference is that now the degrees of freedom and the corresponding "level of non-conformity" of the method vary from edge to edge. This approach is similar to that discussed in [18] for the *hp*-version of the conforming standard VEM.

Under this construction, one should be able to prove the following convergence result in terms of the number of degrees of freedom. There exists $\mu > 0$ such that the choice (61) guarantees

$$|u - u_n|_{1,\mathcal{T}_n} \leq c \exp\left(-b \sqrt[2]{\#\text{dofs}}\right), \tag{62}$$

for some positive constants b and c, depending on u, ρ_1, ρ_2, Λ, and σ, where #dofs denotes the number of degrees of freedom of the discretization space. This exponential convergence in terms of the dimension of the approximation space was proven for conforming harmonic VEM in [36] and for Trefftz DG-FEM in [45]. In the present non-conforming harmonic VEM, the setting of the proof of such exponential convergence would follow the same lines as that of the two methods mentioned above. We omit a detailed analysis and present here some numerical results.

We underline that the exponential convergence in (62) is faster (in terms of the dimension of the space) than that of standard *hp*-FEM [56] and *hp*-VEM [18], whose decay rate is

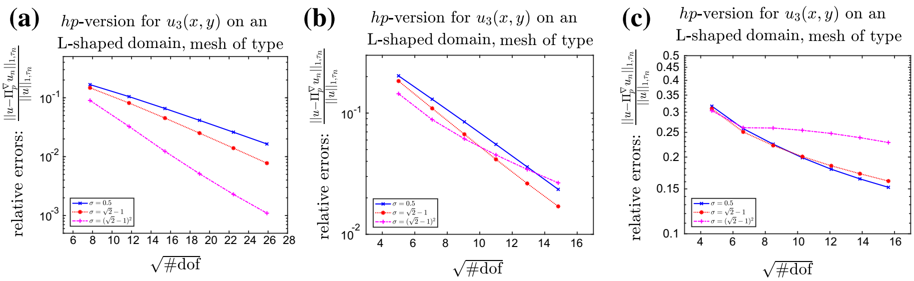

Fig. 7 Convergence of the hp-version of the method for the solution u_3 on an L-shaped domain Ω, for the three sequences of graded meshes represented in Fig. 6; relative H^1 errors defined in (58). The grading parameter σ is set to $1/2$, $\sqrt{2}-1$ and $(\sqrt{2}-1)^2$

$\mathcal{O}(\exp\left(-b\sqrt[3]{\#\text{dofs}}\right))$, due to the use of harmonic subspaces instead of complete FE or VE spaces.

For our numerical tests, we consider the boundary value problems (2) on the L-shaped domain Ω defined in (60), with exact solution

$$u_3(x, y) = u_3(r, \theta) = r^{\frac{2}{3}} \sin\left(\frac{2}{3}\theta + \frac{\pi}{3}\right).$$

We note that $u_3 \in H^{\frac{5}{3}-\epsilon}(\Omega)$ for every $\epsilon > 0$ arbitrarily small, and also $u_3 \in H^{\frac{5}{3}-\epsilon}(\Omega_{\text{ext}})$, where Ω_{ext} is defined in (40); we stress that u_3 is the natural solution, singular at $\mathbf{0} = (0, 0)$, which arises when solving a Poisson problem in the L-shaped domain Ω.

In Fig. 7, we show the convergence of the hp-version of the method for different values of the grading parameter σ used in (59) and with degrees of accuracy graded according to (61), having set $\mu = 1$. We plot the logarithm of the relative H^1 error (58) against the square root of the number of degrees of freedom.

Note that, due to the different number of degrees of freedom for each type of mesh, the range of the coordinates varies from plot to plot. The straight lines for $\sigma = 0.5$ and $\sigma = \sqrt{2}-1$ indicate agreement with (62) for meshes of type (a) and (b). However, when employing the mesh of type (c) with all grading parameters, and when employing grading parameter $\sigma = (\sqrt{2}-1)^2$ for meshes of all types, we do not observe exponential convergence (62). In the former case, we deem that this is due to the shape of the elements, whereas, in the latter, this could be due to the fact that the size of the elements in the outer layers is too large if picking the parameter μ in (61) equal to 1.

We point out that, in the framework of the conforming harmonic VEM [36], a similar behaviour for the mesh of type (c) was observed. Instead, when employing the hp-version of the standard (non-harmonic) VEM [18], the performance is more robust and the decay of the error is always straight exponential. This suboptimal behaviour might be intrinsic in the use of harmonic polynomials, or might be due to the choice of the harmonic polynomial basis employed in the construction of the method, see "Appendix A".

5 Conclusions

In this paper, we investigated non-conforming harmonic VEM for the approximation of solutions to 2D Dirichlet–Laplace problems, providing error bounds in terms both of h, the mesh size, and of p, the degree of accuracy of the method. We gave some hints concerning the extension of the method to the 3D case, where the design of a suitable stabilization is the only missing item. Numerical tests validating the theoretical convergence results, as well as testing the hp-version of the method in presence of corner singularities, were presented.

The technology herein introduced can also be seen as an intermediate step towards the construction of non-conforming Trefftz-VE spaces for the approximation of solutions to Helmholtz problems, which has been recently investigated in [49].

Acknowledgements The authors have been funded by the Austrian Science Fund (FWF) through the projects P 29197-N32 and F 65. They are very grateful to the anonymous referees for their valuable and constructive comments, which have contributed to the improvement of the paper.

Appendix A: Details on the Implementation

In this section, we discuss some practical aspects concerning the implementation of the non-conforming harmonic VEM in 2D. We employ henceforth the notation of [16]. It is worth to underline that we present herein only the case with uniform degree of accuracy; the implementation of the hp version is dealt with similarly. As a first step, we begin by fixing the notation for the various bases instrumental for the construction of the method.

Basis of $\mathbb{P}_{p-1}(e)$ for a given $e \in \mathcal{E}^K$. Using the same notation as in (12), we denote the basis of $\mathbb{P}_{p-1}(e)$, $e \in \mathcal{E}^K$, by $\{m_r^e\}_{r=0,\dots,p-1}$. The choice we make is

$$m_r^e(\mathbf{x}) := \mathbb{L}_r\left(\phi_e^{-1}(\mathbf{x})\right) \quad \forall r = 0, \dots, p-1, \tag{63}$$

where $\phi_e : [-1, 1] \to e$ is the linear transformation mapping the interval $[-1, 1]$ to the edge e, and $\mathbb{L}_r$ is the Legendre polynomial of degree r over $[-1, 1]$. We recall, see e.g. [56], for future use the orthogonality property

$$\left(m_r^e, m_s^e\right)_{0,e} = \frac{h_e}{2}\int_{-1}^{1} \mathbb{L}_r(t)\mathbb{L}_s(t)\,\mathrm{d}t = \frac{h_e}{2r+1}\delta_{rs} \quad \forall r, s = 0, \dots, p-1, \tag{64}$$

where δ_{rs} is the Kronecker delta (1 if $r = s$, 0 otherwise).

Basis of $\mathbb{H}_p(K)$ for a given $K \in \mathcal{T}_n$. We denote the basis of the space of harmonic polynomials $\mathbb{H}_p(K)$ by $\{q_\alpha^\Delta\}_{\alpha=1,\dots,n_p^\Delta}$, where $n_p^\Delta := \dim \mathbb{H}_p(K) = 2p + 1$. The choice we make for this basis is

$$q_1^\Delta(\mathbf{x}) = 1;$$

$$q_{2l}^\Delta(\mathbf{x}) = \sum_{k=1,\,k\text{ odd}}^{l} (-1)^{\frac{k-1}{2}} \binom{l}{k} \left(\frac{x - x_K}{h_K}\right)^{l-k} \left(\frac{y - y_K}{h_K}\right)^{k} \quad \forall l = 1, \dots, p;$$

$$q_{2l+1}^\Delta(\mathbf{x}) = \sum_{k=0,\,k\text{ even}}^{l} (-1)^{\frac{k}{2}} \binom{l}{k} \left(\frac{x - x_K}{h_K}\right)^{l-k} \left(\frac{y - y_K}{h_K}\right)^{k} \quad \forall l = 1, \dots, p.$$

The fact that this is actually a basis for $\mathbb{H}_p(K)$ is proven, e.g., in [6, Theorem 5.24].

Basis for $V^\Delta(K)$ for a given $K \in \mathcal{T}_n$. For this local VE space introduced in (11), we employ the canonical basis $\left\{\varphi_{j,r}\right\}_{\substack{j=1,\dots,N_K\\ r=0,\dots,p-1}}$ defined though (13), where we also recall that N_K denotes the number of edges of K.

In the following, we derive the matrix representation of the local discrete bilinear form introduced in (23). We begin with the computation of the matrix representation of the projector $\Pi_p^{\nabla,K}$ acting from $V(K)$ to $\mathbb{H}_p(K)$ and defined in (15). To this purpose, given any basis function $\varphi_{j,r} \in V^{\Delta}(K)$, $j = 1, \ldots, N_K$, $r = 0, \ldots, p-1$, we expand $\Pi_p^{\nabla,K}\varphi_{j,r}$ in terms of basis $\{q_\alpha^{\Delta}\}_{\alpha=1,\ldots,n_p^{\Delta}}$ of $\mathbb{H}_p(K)$, i.e.,

$$\Pi_p^{\nabla,K}\varphi_{j,r} = \sum_{\alpha=1}^{n_p^{\Delta}} s_\alpha^{(j,r)} q_\alpha^{\Delta}. \tag{65}$$

Using (15) and testing (65) with functions q_β^{Δ}, $\beta = 1, \ldots, n_p^{\Delta}$, we get that the coefficients $s_\alpha^{(j,r)}$ can be computed by solving for $\boldsymbol{s}^{(j,r)} := [s_1^{(j,r)}, \ldots, s_{n_p^{\Delta}}^{(j,r)}]^T$ the $n_p^{\Delta} \times n_p^{\Delta}$ algebraic linear system

$$\boldsymbol{G}\boldsymbol{s}^{(j,r)} = \boldsymbol{b}^{(j,r)},$$

where

$$\boldsymbol{G} = \begin{bmatrix} \left(q_1^{\Delta}, 1\right)_{0,\partial K} & \left(q_2^{\Delta}, 1\right)_{0,\partial K} & \cdots & \left(q_{n_p^{\Delta}}^{\Delta}, 1\right)_{0,\partial K} \\ 0 & \left(\nabla q_2^{\Delta}, \nabla q_2^{\Delta}\right)_{0,K} & \cdots & \left(\nabla q_{n_p^{\Delta}}^{\Delta}, \nabla q_2^{\Delta}\right)_{0,K} \\ \vdots & \vdots & \ddots & \vdots \\ 0 & \left(\nabla q_{n_p^{\Delta}}^{\Delta}, \nabla q_2^{\Delta}\right)_{0,K} & \cdots & \left(\nabla q_{n_p^{\Delta}}^{\Delta}, \nabla q_{n_p^{\Delta}}^{\Delta}\right)_{0,K} \end{bmatrix},$$

$$\boldsymbol{b}^{(j,r)} = \begin{bmatrix} \left(\varphi_{j,r}, 1\right)_{0,\partial K} \\ \left(\nabla\varphi_{j,r}, \nabla q_2^{\Delta}\right)_{0,K} \\ \vdots \\ \left(\nabla\varphi_{j,r}, \nabla q_{n_p^{\Delta}}^{\Delta}\right)_{0,K} \end{bmatrix}.$$

Collecting all the $N_K p$ (column) vectors $\boldsymbol{b}^{(j,r)}$ in a matrix $\boldsymbol{B} \in \mathbb{R}^{n_p^{\Delta} \times N_K p}$, namely, setting $\boldsymbol{B} := [\boldsymbol{b}^{(1,1)}, \ldots, \boldsymbol{b}^{(N_K,p)}]$, the matrix representation $\boldsymbol{\Pi}_*$ of the projector $\Pi_p^{\nabla,K}$ acting from $V^{\Delta}(K)$ to $\mathbb{H}_p(K)$ is given by

$$\boldsymbol{\Pi}_* = \boldsymbol{G}^{-1}\boldsymbol{B} \in \mathbb{R}^{n_p^{\Delta} \times N_K p}.$$

Subsequently, we define

$$\boldsymbol{D} := \begin{bmatrix} \mathrm{dof}_{1,1}\left(q_1^{\Delta}\right) & \cdots & \mathrm{dof}_{1,1}\left(q_{n_p^{\Delta}}^{\Delta}\right) \\ \vdots & \ddots & \vdots \\ \mathrm{dof}_{N_K,p}\left(q_1^{\Delta}\right) & \cdots & \mathrm{dof}_{N_K,p}\left(q_{n_p^{\Delta}}^{\Delta}\right) \end{bmatrix} \in \mathbb{R}^{N_K p \times n_p^{\Delta}}.$$

Let $\boldsymbol{\Pi}$ be the matrix representation of the operator $\Pi_p^{\nabla,K}$ seen now as a map from $V^{\Delta}(K)$ into $V^{\Delta}(K) \supseteq \mathbb{H}_p(K)$. Then, following [16], it is possible to show that

$$\boldsymbol{\Pi} = \boldsymbol{D}\boldsymbol{G}^{-1}\boldsymbol{B} \in \mathbb{R}^{N_K p \times N_K p}.$$

Next, denoting by $\widetilde{\boldsymbol{G}} \in \mathbb{R}^{n_p^\Delta \times n_p^\Delta}$ the matrix coinciding with $\boldsymbol{G}$ apart from the first row which is set to zero, the matrix representation of the bilinear form in (23) is

$$(\boldsymbol{\Pi}_*)^T \ \widetilde{\boldsymbol{G}} \ (\boldsymbol{\Pi}_*) + (\boldsymbol{I} - \boldsymbol{\Pi})^T \ \boldsymbol{S} \ (\boldsymbol{I} - \boldsymbol{\Pi})\,.$$

Here, $\boldsymbol{S}$ denotes the matrix representation of an explicit stabilization $S^K(\cdot,\cdot)$. For the stabilization defined in (28), we have

$$\boldsymbol{S}((k-1)N_K + r, (l-1)N_K + s) = \sum_{i=1}^{N_K} \frac{p}{h_{e_i}} \left(\Pi_{p-1}^{0,e_i} \varphi_{l,s}, \Pi_{p-1}^{0,e_i} \varphi_{k,r} \right)_{0,e_i}$$
$$\forall k, l = 1, \dots, N_K, \forall r, s = 0, \dots, p-1.$$

By expanding $\Pi_{p-1}^{0,e_i}\varphi_{l,s}$ and $\Pi_{p-1}^{0,e_i}\varphi_{k,r}$ in the basis $\{m_\gamma^{e_i}\}_{\gamma=0,\dots,p-1}$ of $\mathbb{P}_{p-1}(e_i)$, i.e.,

$$\Pi_{p-1}^{0,e_i}\varphi_{l,s} = \sum_{\gamma=0}^{p-1} t_\gamma^{(l,s),e_i} m_\gamma^{e_i}, \quad \Pi_{p-1}^{0,e_i}\varphi_{k,r} = \sum_{\zeta=0}^{p-1} t_\zeta^{(k,r),e_i} m_\zeta^{e_i},$$
$$\forall k, l = 1, \dots, N_K, \ \forall r, s = 0, \dots, p-1, \tag{66}$$

we can write

$$\boldsymbol{S}((k-1)N_K + r, (l-1)N_K + s) = \sum_{i=1}^{N_K} \sum_{\gamma=0}^{p-1} \sum_{\zeta=0}^{p-1} t_\gamma^{(l,s),e_i} t_\zeta^{(k,r),e_i} \frac{p}{h_{e_i}} \left(m_\gamma^{e_i}, m_\zeta^{e_i} \right)_{0,e_i}$$
$$\forall k, l = 1, \dots, N_K, \ \forall r, s = 0, \dots, p-1.$$

For the basis defined in (63), using the orthogonality of the Legendre polynomials (64), this expression can be simplified leading to a diagonal stability matrix $\mathbf{S}$:

$$\boldsymbol{S}((k-1)N_K + r, (k-1)N_K + r) = \sum_{i=1}^{N_K} \sum_{\zeta=0}^{p-1} \frac{p}{2r+1} \left(t_\zeta^{(k,r),e_i} \right)^2$$
$$\forall k = 1, \dots, N_K, \ \forall r = 0, \dots, p-1.$$

For fixed $i, k \in \{1, \dots, N_K\}$ and $r \in \{0, \dots, p-1\}$, the coefficients $t_\zeta^{(k,r),e_i}$ are obtained by testing $\Pi_{p-1}^{0,e_i}\varphi_{k,r}$, defined in (66), with $m_\zeta^{e_i}$, $\zeta = 0, \dots, p-1$, and by taking into account the definition of Π_{p-1}^{0,e_i} in (14), the orthogonality relation (64) and the definition of $\varphi_{k,r}$ in (13). This gives

$$t_\zeta^{(k,r),e_i} = \frac{2\zeta+1}{h_{e_i}} \left(\varphi_{k,r}, m_\zeta^{e_i} \right)_{0,e_i} = (2\zeta+1)\delta_{ik}\delta_{r\zeta} \quad \forall \zeta = 0, \dots, p-1.$$

The global system of linear equations corresponding to method (10) is assembled as in the standard non-conforming FEM. Finally, one imposes in a non-conforming fashion the Dirichlet boundary datum g by

$$\int_e u_n q_{p-1}^e \,\mathrm{d}s = \int_e g q_{p-1}^e \,\mathrm{d}s \quad \forall q_{p-1}^e \in \mathbb{P}_{p-1}(e),$$

where, in practice, g is replaced by g_p, see Remark 2.

References

1. Aghili, J., Di Pietro, D., Ruffini, B.: A *hp*-hybrid high-order method for variable diffusion on general meshes. Comput. Methods Appl. Math. **17**(3), 359–376 (2017)
2. Ahmad, B., Alsaedi, A., Brezzi, F., Marini, L.D., Russo, A.: Equivalent projectors for virtual element methods. Comput. Math. Appl. **66**(3), 376–391 (2013)
3. Antonietti, P.F., Beirão da Veiga, L., Scacchi, S., Verani, M.: A $\mathcal{C}^1$ virtual element method for the Cahn–Hilliard equation with polygonal meshes. SIAM J. Numer. Anal. **54**(1), 34–56 (2016)
4. Antonietti, P.F., Mascotto, L., Verani, M.: A multigrid algorithm for the *p*-version of the virtual element method. ESAIM Math. Model. Numer. Anal. **52**(1), 337–364 (2018)
5. Arnold, D.N., Brezzi, F., Cockburn, B., Marini, L.D.: Unified analysis of discontinuous Galerkin methods for elliptic problems. SIAM J. Numer. Anal. **39**(5), 1749–1779 (2002)
6. Axler, S., Bourdon, P., Wade, R.: Harmonic Function Theory. Springer, Berlin (2013)
7. Ayuso, B., Lipnikov, K., Manzini, G.: The nonconforming virtual element method. ESAIM Math. Model. Numer. Anal. **50**(3), 879–904 (2016)
8. Babuška, I., Guo, B.: The *hp* version of the finite element method. Comput. Mech. **1**(1), 21–41 (1986)
9. Babuška, I., Guo, B.Q.: Regularity of the solution of elliptic problems with piecewise analytic data. Part I. Boundary value problems for linear elliptic equation of second order. SIAM J. Math. Anal. **19**(1), 172–203 (1988)
10. Babuška, I., Guo, B.Q.: The *hp* version of the finite element method for domains with curved boundaries. SIAM J. Numer. Anal. **25**(4), 837–861 (1988)
11. Babuška, I., Melenk, J.M.: Approximation with harmonic and generalized harmonic polynomials in the partition of unity method. Comput. Assist. Methods Eng. Sci. **4**, 607–632 (1997)
12. Bank, R.E., Parsania, A., Sauter, S.: Saturation estimates for *hp*-finite element methods. Comput. Vis. Sci. **16**(5), 195–217 (2013)
13. Beirão da Veiga, L., Brezzi, F., Cangiani, A., Manzini, G., Marini, L.D., Russo, A.: Basic principles of virtual element methods. Math. Models Methods Appl. Sci. **23**(01), 199–214 (2013)
14. Beirão da Veiga, L., Brezzi, F., Marini, L.D., Russo, A.: Virtual element method for general second-order elliptic problems on polygonal meshes. Math. Models Methods Appl. Sci. **26**(4), 729–750 (2016)
15. Beirão da Veiga, L., Brezzi, F., Marini, L.D.: Virtual elements for linear elasticity problems. SIAM J. Numer. Anal. **51**(2), 794–812 (2013)
16. Beirão da Veiga, L., Brezzi, F., Marini, L.D., Russo, A.: The hitchhiker's guide to the virtual element method. Math. Models Methods Appl. Sci. **24**(8), 1541–1573 (2014)
17. Beirão da Veiga, L., Chernov, A., Mascotto, L., Russo, A.: Basic principles of *hp* virtual elements on quasiuniform meshes. Math. Models Methods Appl. Sci. **26**(8), 1567–1598 (2016)
18. Beirão da Veiga, L., Chernov, A., Mascotto, L., Russo, A.: Exponential convergence of the *hp* virtual element method with corner singularity. Numer. Math. **138**(3), 581–613 (2018)
19. Beirão da Veiga, L., Lipnikov, K., Manzini, G.: The Mimetic Finite Difference Method for Elliptic Problems. Springer, Berlin (2014)
20. Beirão da Veiga, L., Lovadina, C., Russo, A.: Stability analysis for the virtual element method. Math. Models Methods Appl. Sci. **27**(13), 2557–2594 (2017)
21. Beirão da Veiga, L., Lovadina, C., Vacca, G.: Divergence free virtual elements for the Stokes problem on polygonal meshes. ESAIM Math. Model. Numer. Anal. **51**(2), 509–535 (2017)
22. Beirão da Veiga, L., Manzini, G.: A virtual element method with arbitrary regularity. IMA J. Numer. Anal. **34**(2), 759–781 (2014)
23. Beirão da Veiga, L., Russo, A., Vacca, G.: The virtual element method with curved edges. arxiv:1711.04306, (2017)
24. Benedetto, M.F., Berrone, S., Pieraccini, S., Scialò, S.: The virtual element method for discrete fracture network simulations. Comput. Methods Appl. Mech. Eng. **280**, 135–156 (2014)
25. Bernardi, C., Fiétier, N., Owens, R.G.: An error indicator for mortar element solutions to the Stokes problem. IMA J. Numer. Anal. **21**(4), 857–886 (2001)
26. Bernardi, C., Maday, Y.: Polynomial interpolation results in Sobolev spaces. J. Comput. Appl. Math. **43**(1), 53–80 (1992)
27. Bertoluzza, S., Pennacchio, M., Prada, D.: BDDC and FETI-DP for the virtual element method. Calcolo **54**(4), 1565–1593 (2017)
28. Brenner, S.C.: Poincaré–Friedrichs inequalities for piecewise H^1 functions. SIAM J. Numer. Anal. **41**(1), 306–324 (2003)
29. Brenner, S.C., Guan, Q., Sung, L.Y.: Some estimates for virtual element methods. Comput. Methods Appl. Math. **17**(4), 553–574 (2017)

30. Cangiani, A., Dong, Z., Georgoulis, E.H., Houston, P.: *hp*-version discontinuous Galerkin methods for advection–diffusion–reaction problems on polytopic meshes. ESAIM Math. Model. Numer. Anal. **50**(3), 699–725 (2016)
31. Cangiani, A., Dong, Z., Georgoulis, E .H., Houston, P.: *hp*-Version Discontinuous Galerkin Methods on Polygonal and Polyhedral Meshes. Springer, Cham (2017)
32. Cangiani, A., Georgoulis, E.H., Pryer, T., Sutton, O.J.: A posteriori error estimates for the virtual element method. Numer. Math. **137**(4), 857–893 (2017)
33. Cangiani, A., Gyrya, V., Manzini, G.: The non-conforming virtual element method for the Stokes equations. SIAM J. Numer. Anal. **54**(6), 3411–3435 (2016)
34. Cangiani, A., Manzini, G., Sutton, O.J.: Conforming and nonconforming virtual element methods for elliptic problems. IMA J. Numer. Anal. **37**(3), 1317–1354 (2016)
35. Chernov, A.: Optimal convergence estimates for the trace of the polynomial L^2-projection operator on a simplex. Math. Comput. **81**(278), 765–787 (2012)
36. Chernov, A., Mascotto, L.: The harmonic virtual element method: stabilization and exponential convergence for the Laplace problem on polygonal domains. IMA J. Numer. Anal. (2018). https://doi.org/10.1093/imanum/dry038
37. Ciarlet, P.G., Ciarlet, P., Sauter, S.A., Simian, C.: Intrinsic finite element methods for the computation of fluxes for Poisson's equation. Numer. Math. **132**(3), 433–462 (2016)
38. Cockburn, B., Di Pietro, D.A., Ern, A.: Bridging the hybrid high-order and hybridizable discontinuous Galerkin methods. ESAIM Math. Model. Numer. Anal. **50**(3), 635–650 (2016)
39. Cockburn, B., Gopalakrishnan, J., Lazarov, R.: Unified hybridization of discontinuous Galerkin, mixed, and continuous Galerkin methods for second order elliptic problems. SIAM J. Numer. Anal. **47**(2), 1319–1365 (2009)
40. Dassi, F., Mascotto, L.: Exploring high-order three dimensional virtual elements: bases and stabilizations. Comput. Math. Appl. **75**(9), 3379–3401 (2018)
41. Di Pietro, D.A., Ern, A.: Hybrid high-order methods for variable-diffusion problems on general meshes. C. R. Math. Acad. Sci. Paris **353**(1), 31–34 (2015)
42. Gain, A.L., Paulino, G.H., Leonardo, S.D., Menezes, I.F.M.: Topology optimization using polytopes. Comput. Methods Appl. Mech. Eng. **293**, 411–430 (2015)
43. Gardini, F., Vacca, G.: Virtual element method for second order elliptic eigenvalue problems. IMA J. Numer. Anal. (2017). https://doi.org/10.1093/imanum/drx063
44. Grisvard, P.: Elliptic problems in nonsmooth domains. SIAM **69** (2011)
45. Hiptmair, R., Moiola, A., Perugia, I., Schwab, C.: Approximation by harmonic polynomials in star-shaped domains and exponential convergence of Trefftz *hp*-dGFEM. ESAIM Math. Model. Numer. Anal. **48**(3), 727–752 (2014)
46. Li, F.: On the negative-order norm accuracy of a local-structure-preserving LDG method. J. Sci. Comput. **51**(1), 213–223 (2012)
47. Li, F., Shu, C.-W.: A local-structure-preserving local discontinuous Galerkin method for the Laplace equation. Methods Appl. Anal. **13**(2), 215 (2006)
48. Mascotto, L.: Ill-conditioning in the virtual element method: stabilizations and bases. Numer. Methods Partial Differ. Equ. **34**(4), 1258–1281 (2018)
49. Mascotto, L., Perugia, I., Pichler, A.: A nonconforming Trefftz virtual element method for the Helmholtz problem. arxiv:1805.05634 (2018)
50. Melenk, J.M.: Operator adapted spectral element methods I: harmonic and generalized harmonic polynomials. Numer. Math. **84**(1), 35–69 (1999)
51. Melenk, M.: On Generalized Finite Element Methods. PhD thesis, University of Maryland (1995)
52. Moiola, A.: Trefftz-discontinuous Galerkin methods for time-harmonic wave problems. PhD thesis (2011)
53. Mora, D., Rivera, G., Rodríguez, R.: A virtual element method for the Steklov eigenvalue problem. Math. Models Methods Appl. Sci. **25**(08), 1421–1445 (2015)
54. Perugia, I., Pietra, P., Russo, A.: A plane wave virtual element method for the Helmholtz problem. ESAIM Math. Model. Numer. Anal. **50**(3), 783–808 (2016)
55. Rjasanow, S., Weißer, S.: Higher order BEM-based FEM on polygonal meshes. SIAM J. Numer. Anal. **50**(5), 2357–2378 (2012)
56. Schwab, C.: *p*- and *hp*- Finite Element Methods: Theory and Applications in Solid and Fluid Mechanics. Clarendon Press, Oxford (1998)